Advances in Nano Research, *Vol. 16, No. 1 (2024) 91-109*
https://doi.org/10.12989/anr.2024.16.1.091

Random topological defects in double-walled carbon nanotubes: On characterization and programmable defect-engineering of spatio-mechanical properties

A. Roy[1], K. K. Gupta[2], S. Dey[1] and T. Mukhopadhyay[*3]

[1]*Department of Mechanical Engineering, National Institute of Technology Silchar, Silchar, India*
[2]*Amrita School of Artificial Intelligence, Amrita Vishwa Vidyapeetham, Coimbatore, India*
[3]*Department of Aeronautics and Astronautics, University of Southampton, Southampton, UK*

(*Received May 18, 2022, Revised June 20, 2023, Accepted December 4, 2023*)

Abstract. Carbon nanotubes are drawing wide attention of research communities and several industries due to their versatile capabilities covering mechanical and other multi-physical properties. However, owing to extreme operating conditions of the synthesis process of these nanostructures, they are often imposed with certain inevitable structural deformities such as single vacancy and nanopore defects. These random irregularities limit the intended functionalities of carbon nanotubes severely. In this article, we investigate the mechanical behaviour of double-wall carbon nanotubes (DWCNT) under the influence of arbitrarily distributed single vacancy and nanopore defects in the outer wall, inner wall, and both the walls. Large-scale molecular simulations reveal that the nanopore defects have more detrimental effects on the mechanical behaviour of DWCNTs, while the defects in the inner wall of DWCNTs make the nanostructures more vulnerable to withstand high longitudinal deformation. From a different perspective, to exploit the mechanics of damage for achieving defect-induced shape modulation and region-wise deformation control, we have further explored the localized longitudinal and transverse spatial effects of DWCNT by designing the defects for their regional distribution. The comprehensive numerical results of the present study would lead to the characterization of the critical mechanical properties of DWCNTs under the presence of inevitable intrinsic defects along with the aspect of defect-induced spatial modulation of shapes for prospective applications in a range of nano-electromechanical systems and devices.

Keywords: defect engineering; defect-induced shape modulation; detective DWCNTs; double-wall carbon nanotubes; nanopore defects; single vacancy defect

1. Introduction

Carbon nanotubes (CNTs) are widely regarded as revolutionary nanostructures due to their versatile capabilities covering mechanical and other multi-physical properties, which have been attracting immense attention from the research community over the last few decades along with a range of other nano-scale derivatives of carbon (Rao *et al*. 2018, Mukhopadhyay *et al*. 2017, 2020, Omer *et al*. 2020, Mukherjee *et al*. 2014, Farshad *et al*. 2020, Gupta *et al*. 2023, Saumya *et al*. 2023). Iijima (1991) synthesized the first one-dimensional needle-like carbon structures, which triggered extensive research into CNTs and their applications in various fields of science and engineering due to their exceptional promise of applications in a range of nano-electromechanical systems and devices. Carbon nanotubes are reported as one of the strongest and stiffest materials discovered so far. In this paper, we embark on characterizing the effect of intrinsic defects on the mechanical and spatial geometric properties along with the aspect of defect-induced shape modulation.

Numerous studies have been conducted to understand the mechanical behaviour of CNTs (Gaillard *et al*. 2005, Fu *et al*. 2007, Yao *et al*. 2001, Sun *et al*. 2002, Chandra *et al*. 2022, Liu *et al*. 2011, Dilrukshi *et al*. 2015, Haiquan *et al*. 2021, Tao *et al*. 2021). The exceptional multi-physical properties of these carbon-based nanostructures have made them a promising candidate for a variety of engineering applications, including use as a reinforcement agent in high-performance composites (Chowdhury *et al*. 2007, Li *et al*. 2019, Chawla *et al*. 2017, Merino *et al*. 2017), fabrication of nanosensors, antennas and nano-resonators (Qian *et al*. 2014, El-Sherbiny *et al*. 2013, Dong *et al*. 2018, Eichler *et al*. 2011, Wang *et al*. 2014), electronic transistors (Liu *et al*. 2020, Jinkins *et al*. 2019), nano-composites (Kinloch *et al*. 2018, Khan *et al*. 2016), and so on. The extreme mechanical and physical properties of CNT, such as high thermal conductivity, high strength, and stiffness, have made it an ideal nano-material for the development of nanocomposites. The previous research reports an extensive mechanical characterization of carbon nanotubes by experimental and theoretical studies. For instance, Demczyk *et al*. (2002) used transmission electron microscopy (TEM) to examine the mechanical behaviour of CNTs. They conducted nano-scale tensile and bending tests and discovered that carbon nanotubes could withstand extreme loads and store significant amounts of energy. Using catalytic decomposition of hydrocarbons, Li *et al*. (2000) fabricated a single-walled carbon nanotube (SWCNT) of 20 mm in ength and

*Corresponding author, Ph.D.,
E-mail: T.Mukhopadhyay@soton.ac.uk

ISSN: 2287-237X (Print), 2287-2388 (Online)

conducted tensile tests to calculate the failure stress of the SWCNT. Xie *et al*. (2000) used chemical vapour deposition (CVD) to create long multi-walled carbon nanotubes (MWCNTs) and characterized the structures by using an energy dispersive X-ray system (EDX) and high-resolution experimental microscopes. Salvetat *et al*. (1999) predicted the mechanical characteristics of MWCNTs with the help of atomic force microscopy (AFM) and reported that the modulus of elasticity of MWCNTs depends upon the structural order within the tube walls. Yu *et al*. (2000) measured the mechanical characteristics of multiwalled CNT (MWCNT) utilizing a transmission electron microscope (TEM), while Treacy *et al*. (1996) calculated the modulus of elasticity of isolated SWCNT using a similar method. With the recent advancements in computational technologies, the research community has begun to prefer computational methods such as finite element method (FEM), molecular dynamics (MD) simulation, and density functional theory (DFT) for the characterization of complex nanomaterials. For instance, Rao *et al*. (2015) estimated the armchair, zigzag, and chiral-dependent mechanical properties of SWCNT by utilizing the finite element method. Farazin *et al*. (2020) used MD simulation to examine the diameter-dependent mechanical properties of SWCNTs. Mielke *et al*. (2004) adopted DFT and molecular mechanics to establish the mechanical properties of CNTs. Ogata and Shibutani (2003) analyzed the ideal tensile strength, modulus of elasticity, and band-gap of SWCNTs using DFT and the tight-binding method. Fu *et al*. (2007) performed MD simulations using Brenner potential to explain the atomic interaction in SWCNTs. Yazdani *et al*. (2017) conducted a series of MD simulations on CNTs to examine the influence of chirality, size, aspect ratio, and slenderness ratio on mechanical properties. They also discovered that CNTs with larger diameters fail at lower tensile stress and strain rate. Similarly, Yang *et al*. (2007) calculated the fracture strength of the defected SWCNT by using MD simulation and established the correlation between the length of SWCNT and corresponding fracture strengths. The MWCNT can be perceived as multiple concentric carbon nanotubes nested inside one another. The inter-wall spacing of the MWCNT depends on the chirality indices of the constituent nanotubes (Qian *et al*. 2002).

Previous research on nano-scale carbon materials such as graphene and CNT suggests that their exceptional multi-physical properties are due to the consistent and ideal topology. Even minor structural and topological modifications cause a dramatic change in the properties of pristine nano-materials. These unavoidable structural defects are either formed during synthesis or intentionally induced to regulate the properties of the nano-materials. The possible defects in CNTs comprise single vacancy defects, nanopore defects, Stone-Wales defects, and single adatom defects that arise during the fabrication process. A single vacancy defect (Zhang *et al*. 2021) is formed when a single carbon atom is missing from the hexagonal carbon ring. The nanopore defects (Gupta *et al*. 2020) can be realized due to absence of an entire hexagonal ring of carbon atoms from the structure. Stone-Wales (SW) defects are a form of crystallographic defect that affects the electrical, chemical, and mechanical properties of carbon-based nanomaterials. There is no involvement of any removal or addition of carbon atoms in the case of SW defect. Here four hexagons are transformed into two pentagons and two heptagons by rotating one of the C—C bonds by 90° (Bedi *et al*. 2022). When an additional carbon atom is covalently bonded to two neighboring carbon atoms, it generates the interstitial defect known as single adatom defect. Here, two adjacent hexagonal rings are converted to two heptagonal rings (Lv *et al*. 2017). There are several methods to experimentally synthesize CNT, but one most common method of large-scale commercial production of CNT is chemical vapor deposition (CVD). The CVD process takes place under a very harsh environment which involves elevated temperature and foreign elements in terms of precursors which results in the inclusion of defects in the pristine structure. The most common defects that are produced in the CVD process are single vacancy defect and nanopore defect. In the current paper, we would focus on these two forms of defects. Previously, many researchers accounted for the experimental realization of these structural defects (Robertson *et al*. 2013, Robertson *et al*. 2012, Wang *et al*. 2017, Yin *et al*. 2012). With this understanding, several groups of researchers have investigated the effect of irregularities on the mechanical performance of such carbon nanomaterials. For example, Gupta *et al*. (2020, 2021) used MD simulations to explore the combined influence of defects and foreign elements on the mechanical characteristics of graphene. They discovered that the fracture and elastic behaviour of graphene shows a drastic decline with the increase in nanopore defect concentration compared to the Stone-Wales defect concentration. It was also observed that the combined influence of these defects reveals a sort of intermediate effect. Randomness in the concentration of individual defects also plays a significant role in the physical characteristics of such materials. In this context, a few research groups performed probabilistic defect modelling and analysis. For instance, Gupta *et al*. (2021) presented the stochastic variation in single vacancy concentrations and silicon dopant concentrations to map the uncertain mechanical performance of monolayer graphene in armchair and zigzag edge configuration. Rafiee and Pourazizi (2014) utilized the nanoscale continuum approach to report the influence of randomly applied structural defects on the mechanical behaviour of CNT. Esbati and Irani (2018) investigated the structural reliability of CNT by utilizing stochastic finite element method. They revealed that the reliability of the CNTs greatly relies on the critical defect density. Saxena and Lal (2012) investigated the impact of Stone-Wales and single vacancy defects on the mechanical characteristics of SWCNT by performing the MD simulations. Roy *et al*. (2021) explored the combined influence of single vacancy and nanopore defect on the mechanical performance of SWCNT. They reported that the SWCNT imposed with nanopore defect is more vulnerable as comparison to a single-vacancy defect. Rafiee and Pourazizi (2014) employed the finite element analysis technique to explore the impact of structural irregularities on the mechanical performance of SWCNT. They accounted that with a 2% concentration of vacancy defect,

Young's modulus of SWCNT reduces by 12%. Yaun *et al*. (2012) studied the structural irregularities in CNTs and suggested that incorporating a metal catalyst can heal the structural irregularities profoundly. Ehyaei *et al*. (2017) estimated the natural frequencies of DWCNT with initial imperfections in them. Roy *et al*. (2022) investigated the temperature-dependent vibrational properties of various heterogeneous nanotubes. Etesami *et al*. (2022) reviewed the capabilities and applications of 3D CNT-graphene hybrid structures in different energy-related devices such as batteries and supercapacitors. Jyoti and Singh (2021) reviewed the 3D CNT-graphene structures in terms of their capabilities in producing polymer composites with uniform dispersion in the reinforcement materials. Kuznetsov *et al*. (2014) conducted Raman spectroscopy to investigate defects in MWCNTs and graphene flakes deposited on MWCNTs. Ghavamain *et al*. (2012) used finite element analysis to obtain the mechanical characteristics of defective SWCNTs and MWCNTs. They observed that any irregularities in the pristine structures result in reduced stiffness and lower Young's modulus values. Eftekhari *et al*. (2013) performed a series of MD simulations to explore the buckling behaviour of pristine and defective SWCNTs and MWCNTs. Their study revealed that imperfection in nano-structures largely reduces the buckling stress compared to pristine structures. Seifoori *et al*. (2020) predicted the impact behaviour of MWCNT in the MD environment and observed that, with an increase in the number of walls of MWCNT, the local deformation reduces. Fan *et al*. (2010) used the low-energy ultrasonic treatment on CNTs in hot concentrated hydrochloric acid to make MWCNTs, and further TEM was used to examine the surface morphology.

In the past five years, the concept of creating electrical circuits out of the fundamental building blocks of materials—molecules—has experienced a resurgence. This concept is a significant part of nanotechnology. The connections between switches and other active devices play an increasingly significant role in every electronic circuit, but especially so when circuit dimensions approach to the nanoscale. Their spatial shape morphing ability makes CNTs an ideal candidate for connections in molecular electronics, they have been demonstrated as switches themselves (Dequesnes *et al*. 2004, Yousif *et al*. 2008). Other applications of shape morphing are in flexible electronic devices (Sun *et al*. 2011), thermoelectric devices (Nakai *et al*. 2014, Esfarjani *et al*. 2006), and mechanical strain sensors (Yilmazoglu *et al*. 2012, Cullinan *et al*. 2010). The prospective modulation of different physical properties other than the mechanical attributes are conductance, LDOS (localization of the density of state), current and electronic energy band gap (Ohnishi *et al*. 2016).

As discussed in the preceding paragraphs, owing to extreme operating conditions of the synthesis process of carbon nanostructures, they are often imposed with certain inevitable structural deformities such as single vacancy and nanopore defects. These random irregularities limit the intended functionalities of carbon nanotubes significantly. As concisely presented in this section, the physical and mechanical performances of pristine and defective carbon nanostructures have been widely explored over the last few years. However, even though a combined occurrence of different types of random defects is inevitable and their influence could be more critical compared to the individual effects, the mechanical characteristics of DWCNT under the influence of such combined random defects are not sufficiently explored. Further, there exists a strong rationale to explore the aspect of defect-induced property modulation, wherein localized longitudinal and transverse spatial effects of regionally distributed defects may be exploited for functional shape modulation. A detailed understanding of the mechanical behaviour of defective DWCNTs is critical for their potential applications in a range of nanoscale devices. Hence, in the current research, we would perform a series of MD simulations to extensively probe the combined influence of the nanopore and single vacancy defect on the spatio-mechanical characteristics of DWCNTs.

2. Modelling and simulation

In the present study, atomic-level simulations are used to investigate mechanical features of different nano-tubular structures such as fracture strength, failure strain, Young's modulus, and their post-elastic behaviour. The accuracy of the responses derived from the MD simulations depends on the use of proper force fields. The Tersoff force field is found to be extensively used in literature to characterize carbon-based nanomaterials such as graphene and CNTs (Gupta *et al*. 2020, 2021, Roy *et al*. 2021). Hence, in the present study, the Tersoff force field is utilized to model pristine and defective MWCNT. The nanotubes' mechanical behaviour is assessed by enforcing an iso-strain approach while performing the MD simulations. The approach adopted for modelling and simulation of the structures is explained systematically in the following paragraphs.

The uniaxial deformation of different nano-tubular structures is simulated in the LAMMPS (Plimpton 1995) atmosphere. The inter-atomic interactions between the carbon atoms are catered by the Tersoff force field (Tersoff 1988), wherein the potential energy between two neighboring carbon atoms can be depicted as

$$E = \frac{1}{2}\sum_{i}\sum_{j\neq i} U_{ij} \tag{1}$$

where

$$U_{ij} = F_C(r_{ij})[F_R(r_{ij}) + b_{ij}F_A(r_{ij})] \tag{2}$$

U_{ij} refers to the potential energy between the carbon atoms. F_R and F_A represent the repulsive and attractive couple potentials, while F_C refers to the cut-off function. Eqs. 1 and 2 together represents the potential energy of adjacent atom (j) of atom i in the range of the cut-off radius. The interspace between the adjacent atoms i and j are represented by r_{ij}, and b_{ij} is the bond-order coefficient, while F_R and F_A can be expressed as

$$F_R = A\, e^{-\lambda_1} \tag{3}$$

$$F_A = -B\, e^{-\lambda_2} \quad (4)$$

Here A, B, λ_1, and λ_2 are the variables used for the interaction of two bodies (Plimpton 1995).

In addition to Tersoff's force field, researchers have used other force fields in the past; for example, Jesen *et al*. (2015) used Chenoweth C/H/O parameterized ReaxFF to perform MD simulations and explore the mechanical performance of carbon materials such as diamond, graphene, and CNT. Similarly, Diao *et al*. (2017) used ReaxFF to run MD simulations to estimate the thermal conductivities of graphene and CNT. UFF (Genoese *et al*. 2020), COMPASS (Savin *et al*. 2020), and AIREBO (Sharma *et al*. 2013) have also been used to characterize carbon nanoparticles in the past. However, the literature review suggests that AIREBO and Tersoff are the most widely employed interatomic potentials for simulating carbon nanostructures. As a result, the Tersoff interatomic potential is used to model the various MWCNT structures in the present study. However, a few investigations have suggested that using the Tersoff's original interatomic potential embellishes the mechanical characteristics of carbon-based nanomaterials. Consequently, Lindsay and Broido (2010) developed the optimized Tersoff potential by applying slight alteration in the two variables (h and B) and calculated the phonon scattering data of SWCNTs and graphene. Mortazavi *et al*. (2016) obtained the mechanical characteristics of amorphized graphene by altering the value of the cut-off function of the optimized Tersoff to 0.2nm. In another study, Rajsekaran *et al*. (2016) suggested a modified Tersoff by merging the alteration communicated by Lindsay and Broido (2010) and Mortazavi *et al*. (2016). To remove the inconsistency of the fracture properties of graphene, they proposed a Tersoff interatomic force field with a modified value of cut-off distance. They concluded that the accuracy of the modified Tersoff potential is enhanced with a fixed value of cut-off distance. To explore the uncertainties associated with the Tersoff force field parameters in terms of fracture strength of graphene, Gupta *et al*. (2021) carried out a large-scale data-driven analysis. In the current study, we have opted for optimized Tersoff potential, suggested by Rajsekaran *et al*. (2016), instead of original Tersoff potential.

The inter-wall interaction between the walls of MWCNT is characterized by Lennard-Jones potential (Jones 1924). The global uniaxial stress developed in the nano-tubular structures due to the uniaxial strain rate is determined as the virial component in the LAMMPS environment (Gupta *et al*. 2020, Gupta *et al*. 2021). The virial stresses derived from the simulation in LAMMPS are the product of pressure and volume; hence, the resulting virial stress values are divided by the system's total volume. In this regard, the instantaneous volume is determined as $V_0(1+\varepsilon)$, where V_0 is the system's initial volume, and ε is the instantaneous strain (Gupta *et al*. 2020). The initial volume of the nanotubes is determined by chirality indices (m,n), wherein the relationship between chirality (m,n) and nanotube diameter is provided by (Roy *et al*. 2021)

$$d = \frac{a\sqrt{m^2 + mn + n^2}}{\pi} \quad (5)$$

Table 1 Validation of MD simulation results with the literature

	Fracture strength (GPa)	Failure strain	Y (TPa)
Talukdar *et al*. (2012) MD-REBO	168.24	0.31	0.79
Chen *et al*. (2008) MD-TERSOFF	-	-	1.019
Liew *et al*. (2004) MD-REBO	168	0.281	1.161
Barber *et al*. (2005) AFM	110	-	-
Wong *et al*. (1997) AFM	-	-	1.28
Demczyk *et al*. (2002) TEM	150	0.102	0.9
Peng *et al*. (2008) TEM	101.7 ± 7.2		1.047
Present Study (MD-Tersoff)	177.2	0.1828	1.46

Here a (≈1.42 Å) denotes the bond length between carbon atoms. The volume of CNT with the length l and the thickness t (≈ 3.33 Å) can be deduced as

$$V_0 = \pi d l t \quad (6)$$

For the critical fracture and elastic details, the stress-strain behaviour of the considered system is investigated. The VMD (Visual Molecular Dynamics) program is used to model various nano-tubular structures (with lengths of 10 nm) (Humphrey *et al*. 1996). Avogadro (Hanwell *et al*. 2012) software is used to perform random and strategic positioning of single vacancy and nanopore defects in pristine structures. As previously stated, the systems' uniaxial deformation is carried out in the LAMMPS environment, where the loading direction (z-direction) is enforced with a periodic boundary condition. Before running the simulations, the energy of the modelled structures is minimized using the conjugate gradient method to ensure the stable state of the system. The potential energy of the structure is minimized to relax the structure before performing the nanotubes' tensile deformation. The results were extracted at an iteration time of 1fs (femtoseconds). The energy minimization of structures is performed for 100 picoseconds, wherein the system's potential energy keeps adjusting the atomic coordinates until it reaches the minimum value. Once the structure is relaxed, the MWCNT is subjected to deformation at the temperature of 300K by enforcing the strain rate of 0.001/picoseconds (ps) in the z-direction. The value of strain rate is selected by observing the strain rate-dependent results reported by Gupta *et al*. (2022). The global stress and strain values are recorded at an interval of 100 timesteps, while the complete simulation is performed for 650 ps, leading to the rupture of pristine MWCNT. The atomic trajectories of the uniaxial deformation of the MWCNTs are visualized using the OVITO (Stukowski *et al*. 2009).

3. Results and discussion

Before conducting comprehensive molecular simulations considering various configurations of DWCNT, we have first validated the fracture and elastic properties of pristine

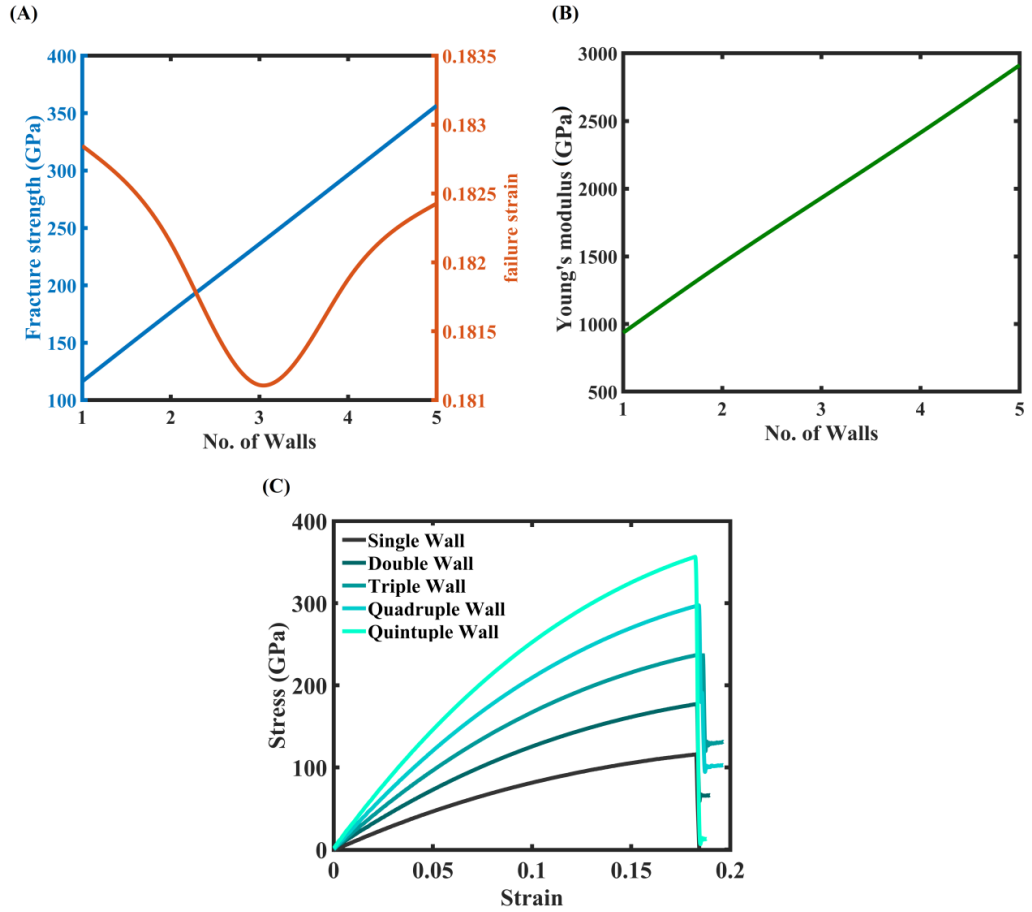

Fig. 1 Number of walls dependent mechanical behaviour of CNTs. (A) Variation of fracture properties with an increasing number of walls (B) Variation of Young's modulus with an increasing number of walls (C) The stress-strain behaviour of MWCNTs

DWCNT with the values published in the literature. In this regard, the uniaxial tensile deformation of a 10 nm long DWCNT (chirality indices of the inner wall (IW): 5, 5; and outer wall (OW): 10, 10) is carried out at 300K temperature under a strain rate of 0.001/ps following the methodology described in the preceding section (Fan *et al*. 2010). The optimized Tersoff force field (Sharma *et al*. 2013) is used to model the interatomic potential between C-C atoms, while the Lennard-Jones potential ($\sigma = 2.4$, and $\varepsilon = 0.00239$) is used to describe the Vander-Waals force between the two walls of DWCNT. The required quantities of interest, such as fracture and elastic characteristics, are found to be consistent with the findings reported in the literature for similar nano-structures (refer to Table 1).

Once enough confidence is gained in the results derived by the MD simulation, we have performed the further analyses presented in the following subsections, wherein the number of walls, temperature, and strain rate dependent fracture and elastic behaviour of DWCNTs is characterized. Further, the DWCNTs are subjected to different scenarios of defect (single vacancy and nanopore) concentration and spatial distribution to assess their influence on the fracture and elastic behaviour of DWCNTs. Along with the influence of individual defect concentration, the present study also illustrates the mechanical behaviour of DWCNTs subjected to combined defect concentrations imposed in both of its walls to comprehensively characterize the vulnerabilities of DWCNTs subjected to uniaxial deformation.

3.1 Uniaxial tensile deformation of perfect MWCNTs

This subsection reports the influence of the number of walls, temperature, and strain rate on the considered nano-tubular structures in a pristine condition. First, the variations in fracture and elastic behaviour of carbon nanotubes are observed with respect to the increase in the number of walls. The CNTs with different numbers of walls (1, 2, 3, 4, and 5) are modelled and uniaxial tensile deformation is performed at room temperature (≈ 300K) with a strain rate of 0.001/ps. Figure 1(A-C) depicts the variation in the mechanical characteristics of MWCNTs with the increase in the number of walls. The findings reveal a significant increase in the tensile strength (≈207%) and Young's modulus (≈213%) of MWCNT, with an increase in the number of walls from one to five. The failure strains corresponding to an increase in the number of walls, on the other hand, do not vary much. Similar trends may also be seen in the stress-strain plots (shown in Fig. 1(C)). Further, a temperature-dependent analysis is performed,

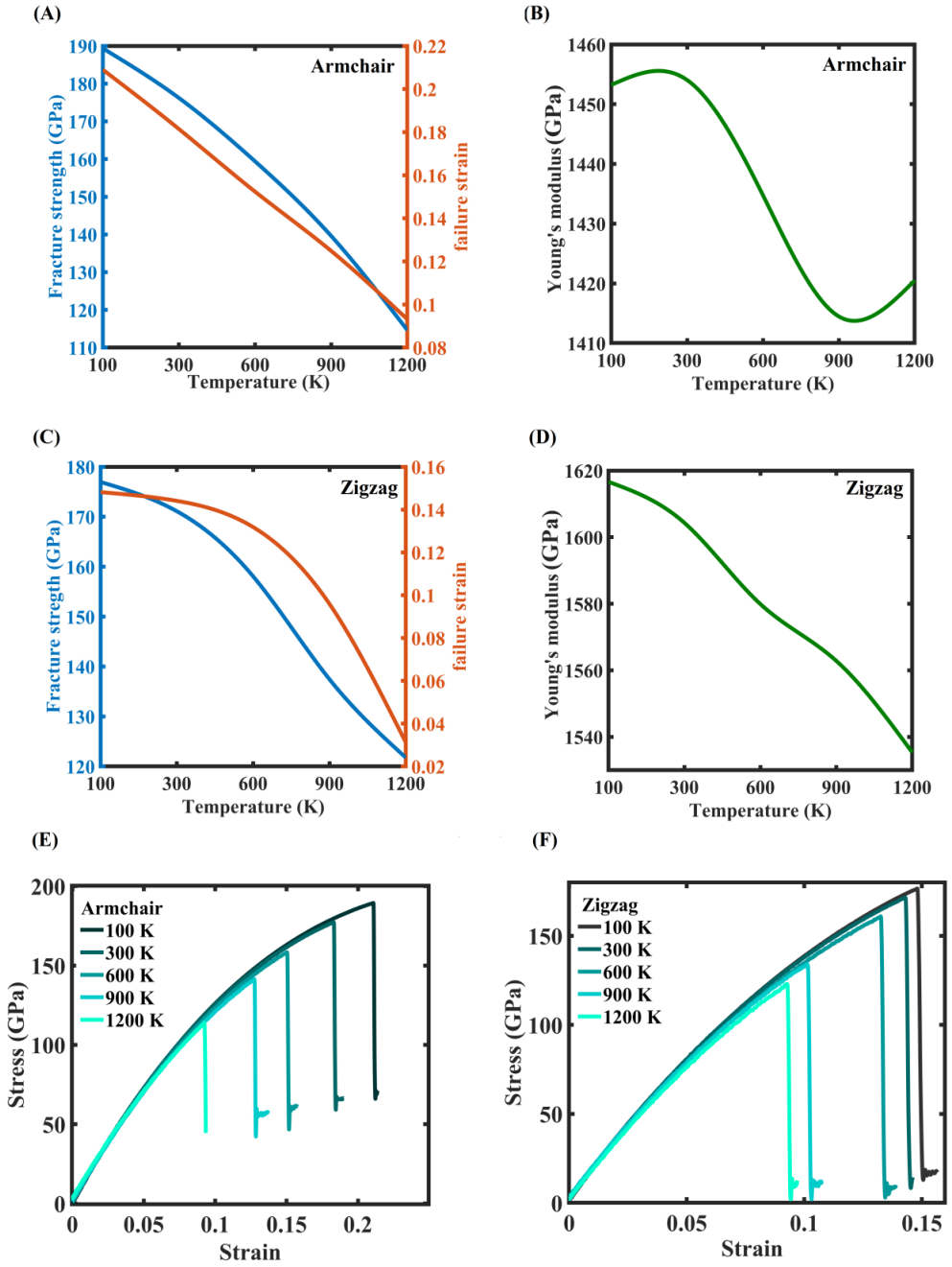

Fig. 2 Temperature-dependent mechanical behaviour of DWCNTs for both the chirality conditions. (A) Variation in fracture characteristics for the armchair direction (B) Variation in elastic behaviour for the armchair direction (C) Variation in fracture characteristics for the zigzag direction (D) Variation in elastic behaviour for the zigzag direction (E) Stress-strain behaviour of DWCNTs in the armchair direction (with increasing temperature) (F) Stress-strain behaviour of DWCNTs in the zigzag direction (with increasing temperature).

wherein the DWCNT is uniaxially deformed with the tensile strain rate of 0.001/ps at different temperatures (100K, 300K, 600K, 900K, and 1200K). The observations derived from the temperature-dependent analysis are illustrated in Fig. 2. The temperature-dependent analysis is performed for both chirality conditions of DWCNT, with the chirality indices for the armchair edge condition set to 10, 10, and 5, 5 for the outer and inner walls, respectively. Similarly, for the zigzag edge conditions, the chirality indices for the outer and inner walls are chosen to be 0, 15, and 0, 10, respectively. The observations drawn from the temperature-dependent analysis reveal that increasing the temperature from 100K to 1200K drastically reduces the mechanical characteristics of DWCNT, regardless of the edge conditions (armchair or zigzag). The variation plots depicted in Fig. 2 (A and B) display that increasing the temperature reduces fracture strength and failure strain by 39.7 % and 55 %, respectively, whereas Young's modulus of DWCNTs shows a little variation (reduced by 1.7%), for the armchair configuration. In the case of a zigzag edge

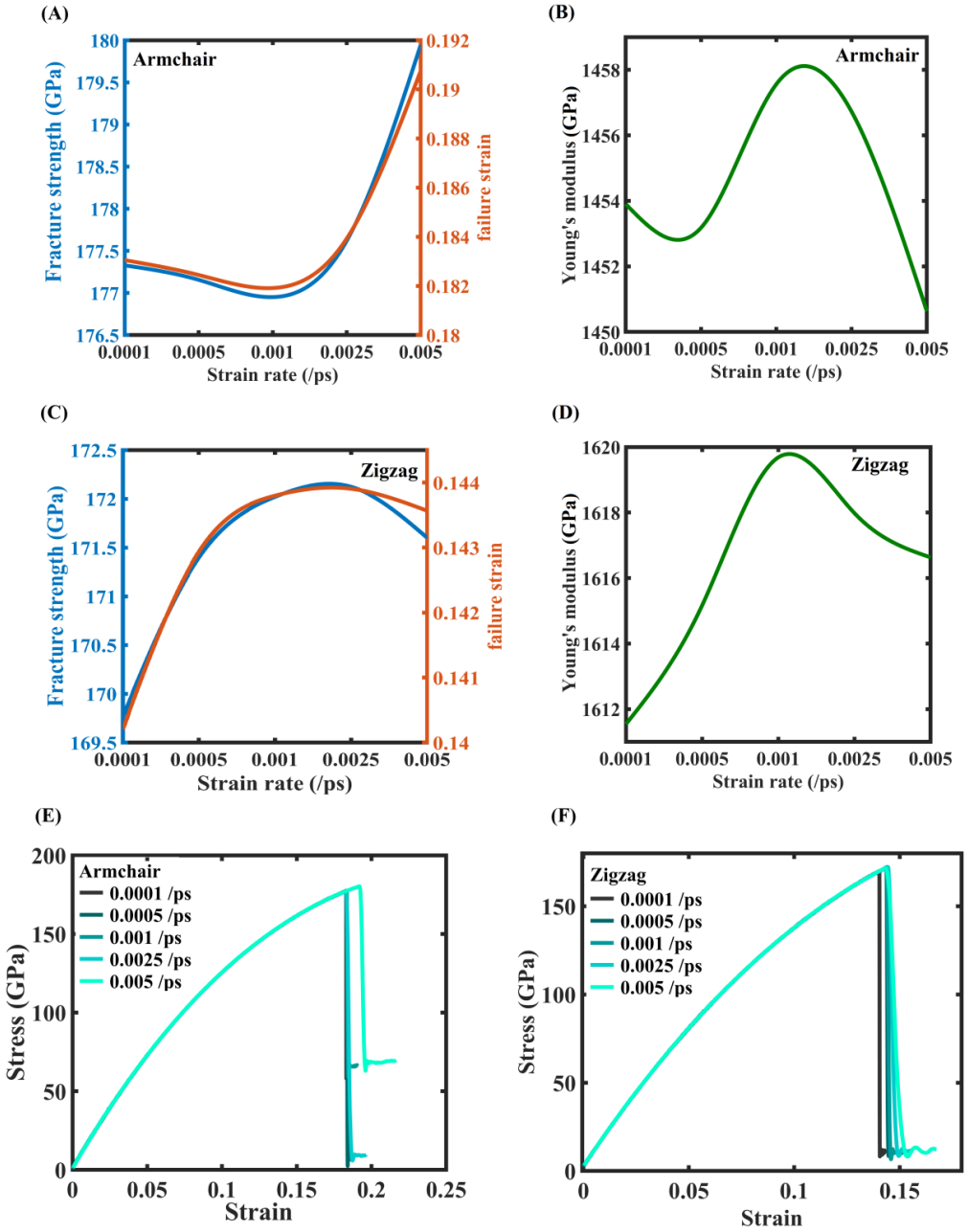

Fig. 3 Mechanical behaviour of DWCNTs with respect to strain rate. (A) Variation in fracture characteristics for the armchair direction (B) Variation in elastic behaviour for the armchair direction (C) Variation in fracture characteristics for the zigzag direction (D) Variation in elastic behaviour for the zigzag direction (E) Strain rate-dependent stress-strain behaviour of DWCNTs in the armchair direction (F) Strain rate-dependent stress-strain behaviour of DWCNTs in the zigzag direction

condition, the fracture strength, failure strain, and Young's modulus are reduced by 30.2 %, 37.15 %, and 5%, respectively (refer to Fig. 2(C-D)). Similar trends can be deduced from the stress-strain behaviour plotted in Fig. 2(E-F).

Keeping in mind that strain rate is a critical factor for nano-scale uniaxial tensile deformation (Gupta *et al*. 2020, 2021a, b, Roy *et al*. 2021), to investigate the effect of variation in strain rate on the fracture and elastic properties of DWCNTs, we have carried out a series of simulations with strain rates varying from 0.0001 /ps to 0.005 /ps with the temperature set at 300K. Similar to the temperature-dependent analysis, the strain rate-dependent analysis is also performed for both chiral edge conditions (armchair and zigzag). The observations drawn from the strain rate dependent analysis are illustrated in Fig. 3, which reveals that regardless of the chiral edge conditions, the fracture and elastic behaviour of DWCNT depict slight changes with the increase in strain rate. For the armchair configuration, the fracture strength, failure strain, and modulus of elasticity vary in the range of 177.3-180.2 GPa, 0.183-0.1915, and 1450-1460 GPa, respectively, while for the zigzag

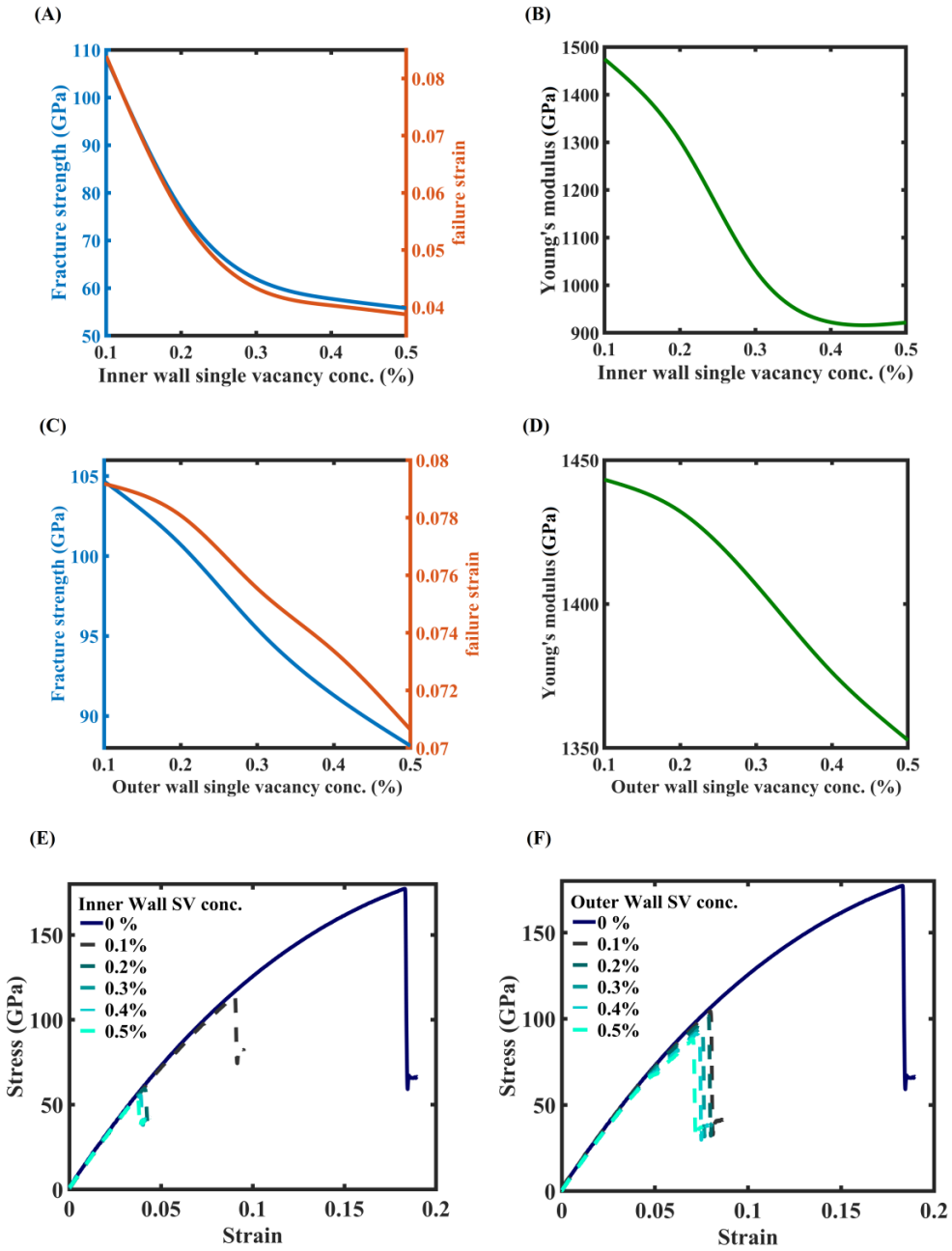

Fig. 4 The effect of single vacancy defect concentrations on the mechanical behaviour of DWCNTs. (A) Variation in fracture characteristics of DWCNT (SV in the inner wall) (B) Variation in Young's modulus of DWCNT (SV in the inner wall) (C) Variation in fracture characteristics of DWCNT (SV in the outer wall) (D) Variation in Young's modulus of DWCNT (SV in the outer wall) (E) Stress-strain behaviour of DWCNT (SV in the inner wall) (F) Stress-strain behaviour of DWCNT (SV in the outer wall). Note that SV stands for single vacancy defect

configuration it varies in the range of 169.6-172.3 GPa, 0.1399-0.1435, and 1612-1617 GPa, respectively.

3.2 Fracture and elastic behaviour of single vacancy defected DWCNT

3.2.1 Single vacancy concentrations in the inner wall

The impact of a single vacancy concentration in the inner wall of the DWCNT on fracture and elastic behaviour is discussed in this subsection. We induce various proportions (0.1% - 0.5%) of single vacancy defects (randomly distributed) in the inner wall of DWCNT to investigate the effects of arbitrary atomic vacancy placement on the mechanical properties of the material (armchair edge condition with chirality indices OW: 10, 10; IW: 5, 5). At a temperature of 300K and a strain rate of 0.001/ps, MD simulations of tensile deformation are carried out. The defects are induced in the armchair edge configureations of DWCNT because the zigzag edge configuration follows the same trend as the armchair edge configurations (as established in previous subsections). Fig. 4 (A, B and E) depicts the variation in the characteristics of DWCNT

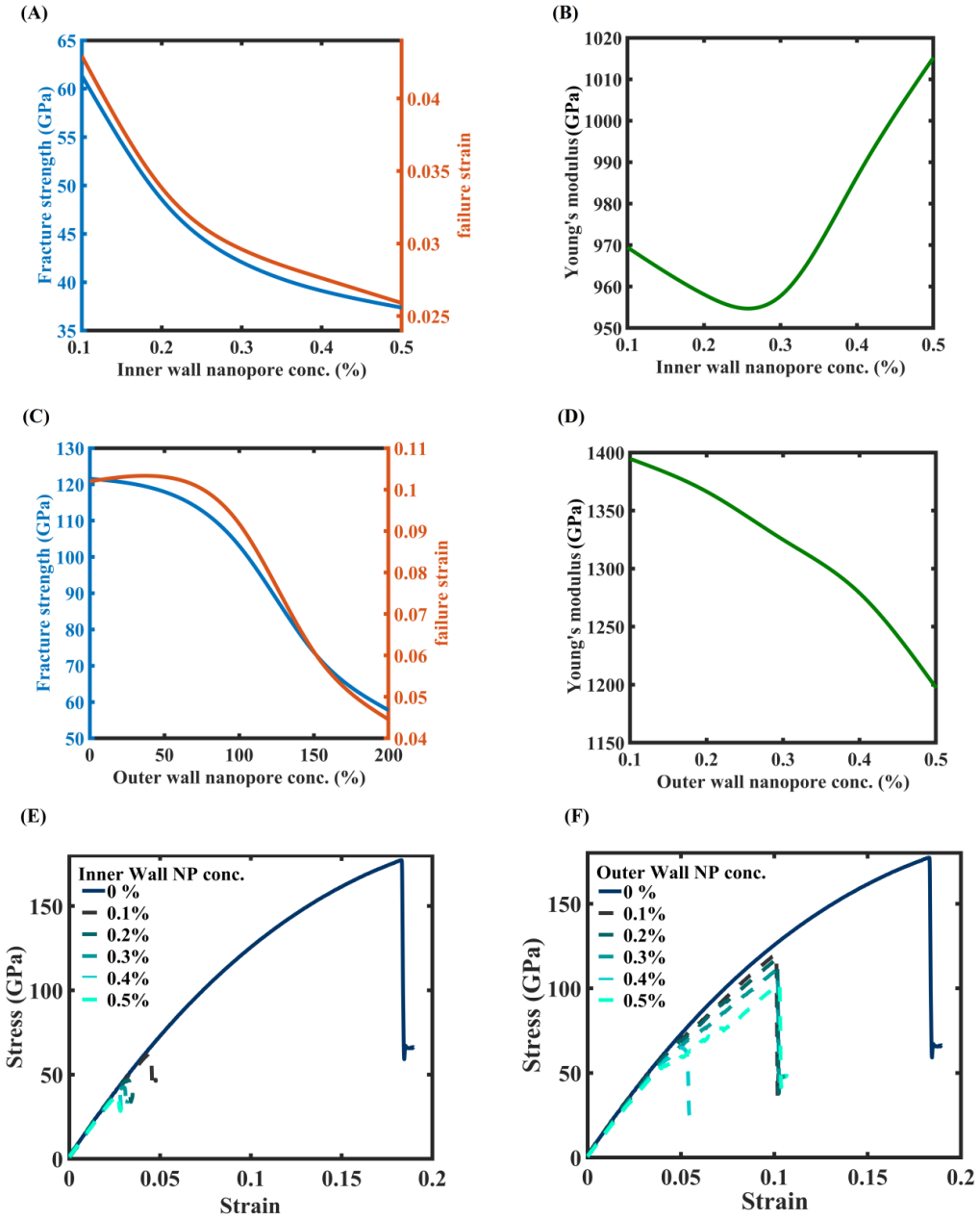

Fig. 5 The effect of nanopore concentrations on the mechanical behaviour of DWCNTs. (A) Variation in fracture characteristics of DWCNT (NP in the inner wall) (B) Variation in Young's modulus of DWCNT (NP in the inner wall) (C) Variation in fracture characteristics of DWCNT (NP in the outer wall) (D) Variation in Young's modulus of DWCNT (NP in the outer wall) (E) Stress-strain behaviour of DWCNT (NP in the inner wall) (F) Stress-strain behaviour of DWCNT (NP in the outer wall). Here NP stands for nanopore defects

corresponding to the increase in defect concentration in the inner wall. When compared to pristine DWCNT, an increase in single vacancy concentrations in the inner wall of DWCNT results in a substantial decrement in the mechanical characteristics, with failure stress, failure strain, and Young's modulus decreasing by 68.5 %, 78.8 %, and 36.16 %, respectively.

3.2.2 Single vacancy concentrations in the outer wall

The observations pertaining to the influence of single vacancy concentrations (0.1 % - 0.5 %) induced in the outer wall of the DWCNT on its mechanical behaviour are reported in this subsection. The findings of defective outer wall-based mechanical behaviour are depicted in Fig. 4 (C, D and F). It can be revealed by observing figure 4, that the defective inner wall makes the DWCNT more vulnerable than the defective outer wall. However, when compared to pristine DWCNT, an increase in single vacancy concentrations in the outer wall of DWCNT results in a significant reduction in fracture properties, with failure stress, failure strain, and Young's modulus decreasing by 50.2 %, 61.4 %, and 7.2 %, respectively. Note that, similar to the cases of the defective inner wall, the single vacancy defects in the outer wall are also placed randomly.

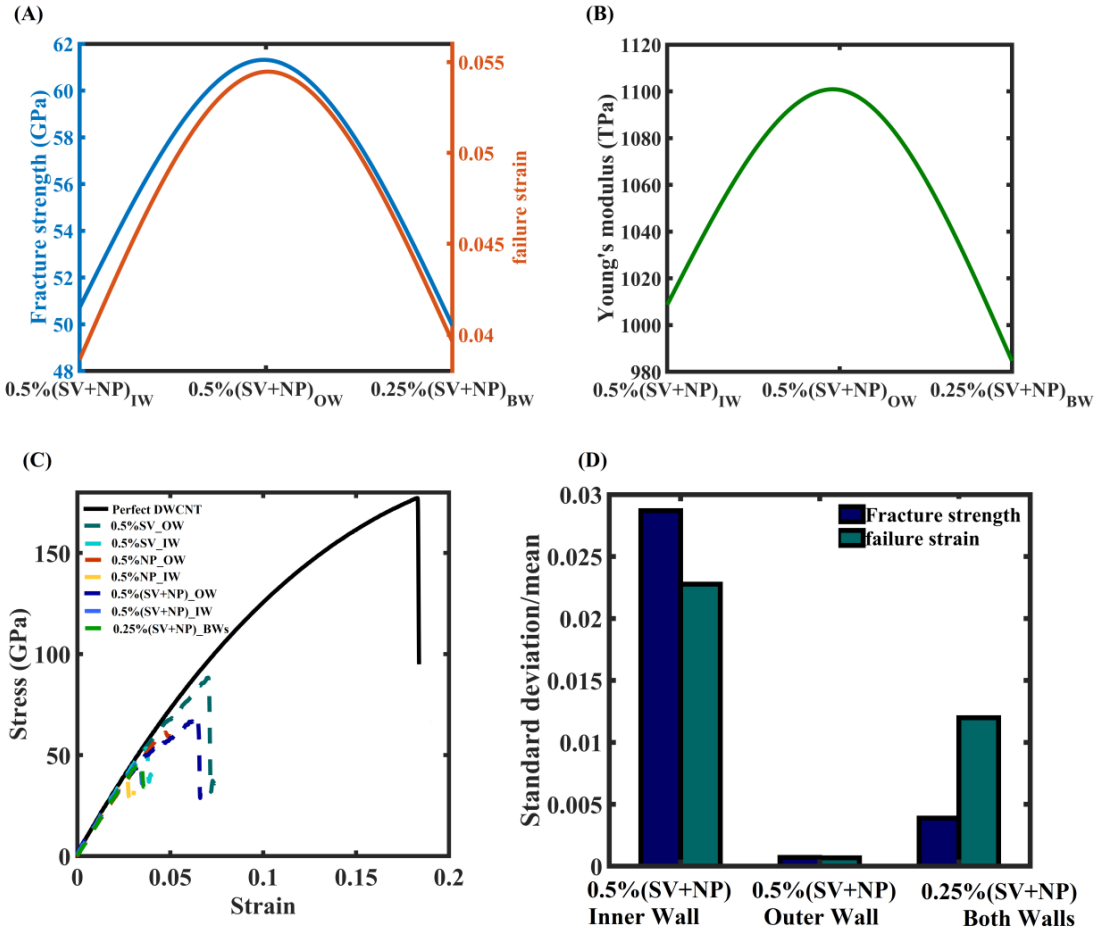

Fig. 6 Wall-specific effect of compound defects concentration on the mechanical behaviour of DWCNT. (A) Variation in fracture characteristics with respect to the imposition of compound defects in the inner wall, outer wall, and both walls of DWCNTs (B) Variation in Young's modulus with respect to the imposition of compound defects in the inner wall, outer wall, and both walls of DWCNTs (C) The comparison of stress-strain behaviour of different cases of defects concentration (D) Variance of fracture strength and failure strain produced by running ten individual molecular simulations of three different compound cases. Note that we did not find any deviation in the corresponding Young's modulus results

3.3 Fracture and elastic behaviour of nanopore defected DWCNT

3.3.1 Nanopore concentrations in the inner wall

This subsection outlines how nanopore defects in the inner wall of DWCNT influence its mechanical behaviour. To evaluate the corresponding tensile strength, failure strain, and modulus of elasticity, the inner wall of the DWCNT is subjected to the nanopore defects in the same proportion (0.1% - 0.5%) as single vacancy defects. The observations drawn from the defective inner wall-based simulations are depicted in Fig. 5 (A, B and E). It is evident from the results that the change of nanopore defect concentrations (from 0.1% to 0.5%) causes a 78.8%, 85%, and 30.5% decrease in failure stress, failure strain, and modulus of elasticity, respectively.

3.3.2 Nanopore concentrations in the outer wall

Fig. 5 (C, D and F) depicts the observations corresponding to the nanopore defective outer wall DWCNTs. The nanopore concentrations in the outer wall of DWCNT are less detrimental when compared to the defective inner wall, similar to the single vacancy defects in the outer wall. The presence of nanopores in the outer wall of DWCNT, on the contrary, indicates a significant drop in mechanical characteristics of DWCNT when compared to its pristine form. When the nanopore defect concentration is altered from 0.1 % to 0.5 %, the failure stress, failure strain, and modulus of elasticity are reduced by 65.7 %, 73.79 %, and 18.42 %, respectively, compared to the pristine DWCNT. In general, Fig. 5 reveals that increasing concentrations of nanopore defects substantially reduce the mechanical properties of DWCNT compared to single vacancy defects. The significant decrease in the fracture properties of DWCNT can be attributed to the sense that nanopore defect behaves as a stress riser which propagates the fracture and leads to early failure of nanotubes.

3.3.3 Mechanical behaviour of DWCNT subjected to compound defects

As discussed in the preceding sections, the occurrence of defects is a result of the CNT synthesis process in most

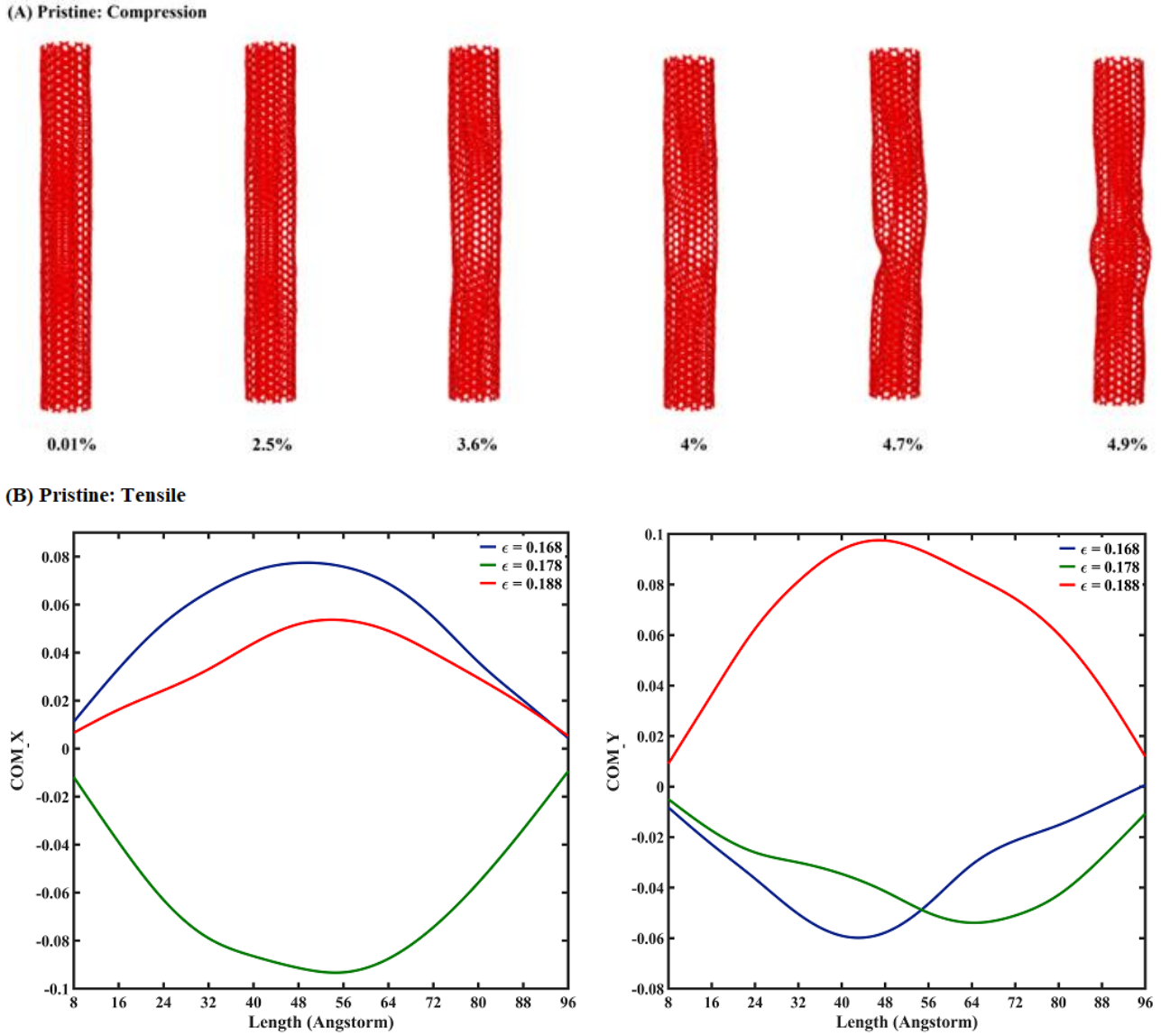

Fig. 7 Shape modulation in pristine DWCNTs. (A) Case of compression (B) Case of tension. Here COM_X and COM_Y in Fig. 7(B) represent the center of masses of atoms in the X and Y direction, respectively

cases. Hence, the synthesized DWCNT may be naturally induced with the single vacancy and nanopore defects in both walls. To investigate the critical combined influence of single vacancy and nanopore defects, a 0.5% concentration of compound defects is first imposed in the inner and outer wall of the DWCNT separately, followed by a 0.25% concentration of compound defects in both walls of the DWCNT. We have also performed a reproducibility analysis for this individual study by running ten individual simulations and observing deviations in predicted results (see Fig. 6(D)). The observations in Fig. 6 reveal that the mechanical behaviour of DWCNT imposed with compound defects in the outer wall is less affected compared to the cases of the inner wall and both walls. The stress-strain relationship confirms the same trend (refer to Fig. 6(C)).

3.4 Spatial modulation of DWCNTs subjected to the region-wise distribution of single vacancy defects

In the preceding sections, we examined the mechanical responses of various cases of DWCNTs in the presence of a random distribution of single vacancy, nanopore defects, and both defects. When compared to single vacancy defects, nanopore defects are found to be more detrimental to the mechanical quantities of interest such as failure stress, failure strain, and Young's modulus. In our previous studies (Gupta *et al.* 2020, Roy *et al.* 2021), the influence of spatially localized positioning of defects is reported on the mechanical performance of carbon-based nanomaterials such as graphene/CNT. The same concentration of defects is intentionally placed at different regions such as top edge, bottom edge or middle of the CNT. It is reported that the nanopore defects at the center of nanotubes cause the most reduction in fracture and elastic properties of SWCNT, followed by the bottom edge, top edge and random distributions, respectively. Thus, it establishes that in addition to defect concentration, the spatial location of

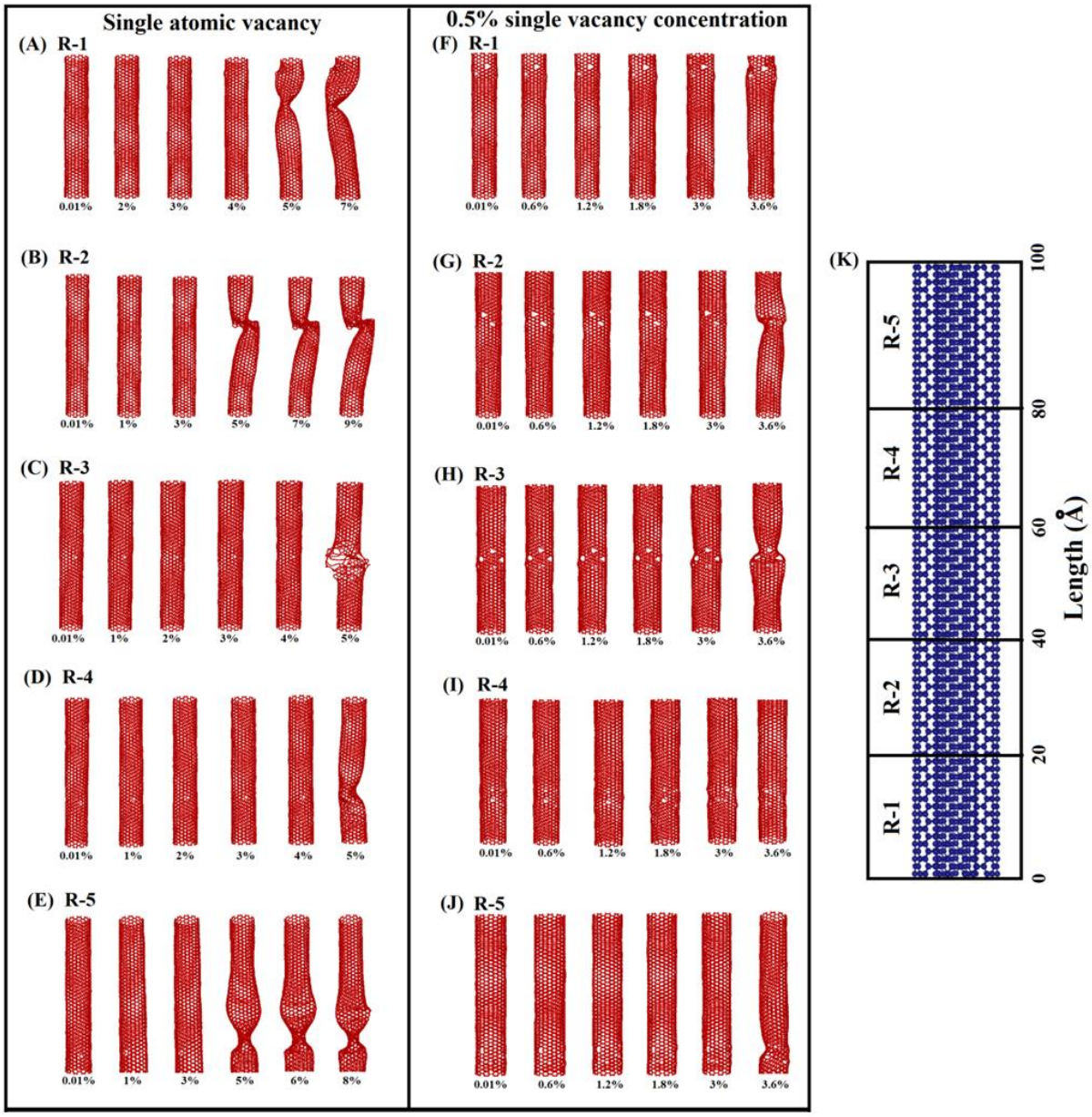

Fig. 8 Spatial shape modulation of DWCNTs under compression. (A-E) The region-wise shape changes under the influence of single atomic vacancy (F-J) The region-wise shape alterations under the influence of 0.5% concentration of single vacancy (K) Regions of the nanotube

defects also influences the mechanical properties of SWCNT. Hence, we further explore the possibility of spatial shape modulation of DWCNTs, as a result of the artificially engineered region-wise distribution of single vacancy defect. The spatial shape modulation (Mukhopadhaya *et al*. 2020) can be realized when the defective nano-structures are uniaxially stretched and compressed. An axial strain rate of 0.001/ps is employed, and the length of two angstroms on both ends of DWCNT is fixed. The defects are imposed region-wise in the outer wall with two different concentrations, single-atom vacancy and 0.5% concentration of single vacancy.

Prior to exploring the defective DWCNTs, the prospect of shape modulation in the pristine DWCNT is analyzed (refer to Fig. 7). The atomic trajectories at different strain percentages reflect the shape modulation of DWCNT during compression, as shown in Figure 7(A). However, the extent (at a particular strain) and location of bulging cannot be controlled in pristine nanotubes, as evident from the figures. Note that the extent of shape changes can be modulated as a function of strain. The cases of tensile deformation of pristine DWCNT do not depict any visual shape alterations laterally, hence the center of mass of atoms with respect to the length of the DWCNT, in the perpendicular directions of the stretching is reported (refer to Fig. 7(B)).

3.4.1 Defective DWCNTs under compression

Under compression, the DWCNT structure reveals localized bulging, primarily at the center of the structure.

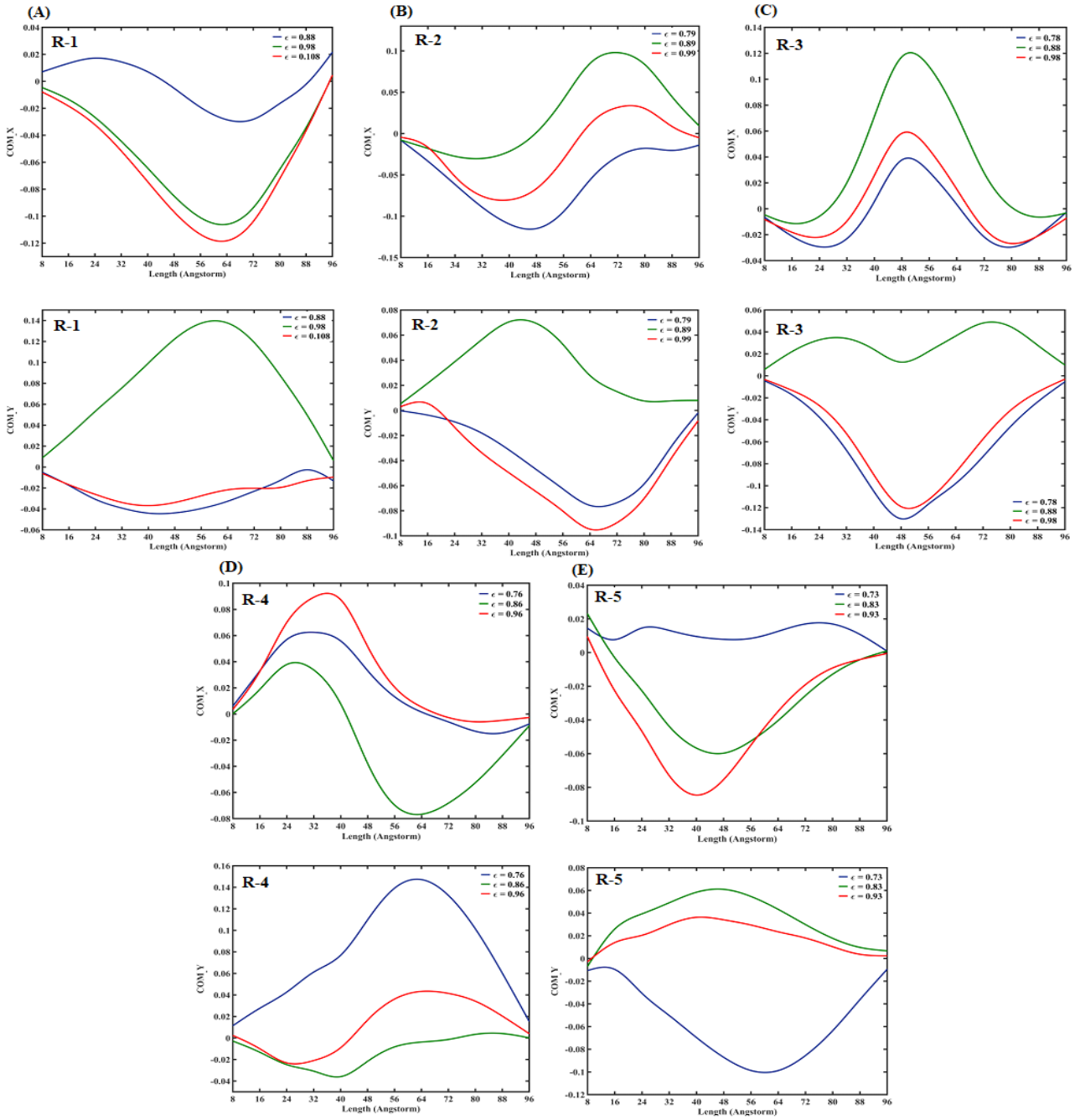

Fig. 9 The lengthwise atomic movement in lateral dimensions of loading with respect to increase in strain for the DWCNT structure imposed with single atomic vacancy. Here COM_X and COM_Y represent the center of mass of atoms in x and y directions respectively. (A) The variation in COM_X and COM_Y for the defect induced in region 1 (B) The variation in COM_X and COM_Y for the defect induced in region 2 (C) The variation in COM_X and COM_Y for the defect induced in region 3 (D) The variation in COM_X and COM_Y for the defect induced in region 4 (E) The variation in COM_X and COM_Y for the defect induced in region 5. The strain values provided in the legend correspond to the strain percentage. The regions are defined in figure 8(K)

To control and modulate the location of the structural shape, the entire length of the tubular structure is divided into five regions of 20-angstrom length each (refer to Fig. 8(K)). The single-atom vacancy is created simultaneously in each region, and structural shape alterations (due to compression) are observed prior to the failure of the structure. The simulations reveal that, aside from the central bulging of the structure, a small amount of spatial change becomes visible in the defective regions (refer to Fig. 8 (A-E)). Considering the small shape modulations in the defected regions of DWCNT structures, in the next step, the concentration of single vacancy defects are increased from single atomic vacancy to 0.5% of vacancy concentrations. It is noteworthy to mention that the increase in the vacancy concentration results in the more controlled phenomenon of shape modulation. The localized shape alteration in the nano-

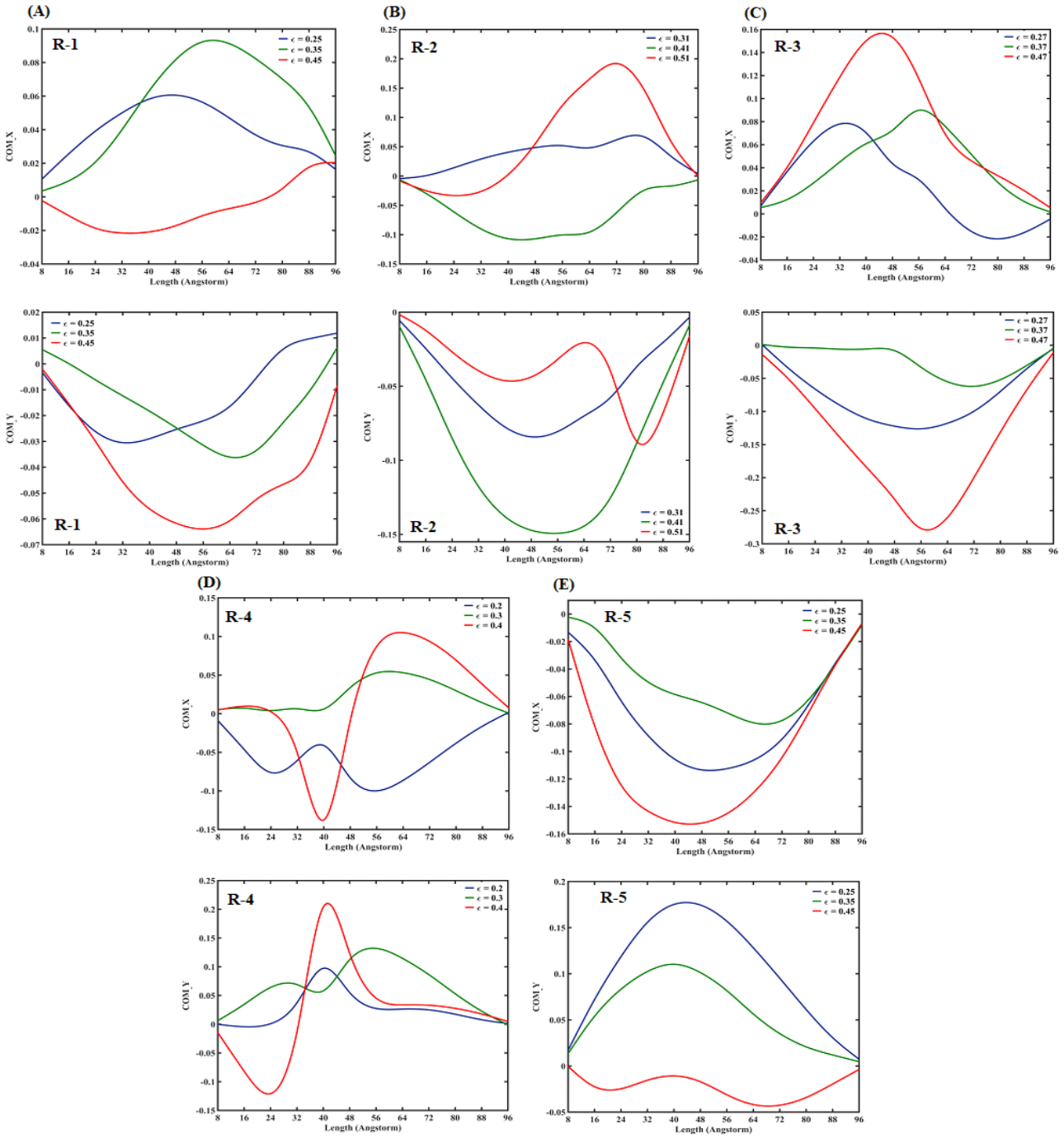

Fig. 10 The lengthwise atomic movement in lateral dimensions of loading with respect to increase in strain for the DWCNT structure imposed with 0.5% single vacancy concentration. Here COM_X and COM_Y represent the center of mass of atoms in x and y directions respectively. (A) The variation in COM_X and COM_Y for the defect induced in region 1 (B) The variation in COM_X and COM_Y for the defect induced in region 2 (C) The variation in COM_X and COM_Y for the defect induced in region 3 (D) The variation in COM_X and COM_Y for the defect induced in region 4 (E) The variation in COM_X and COM_Y for the defect induced in region 5. The strain values provided in the legend correspond to the strain percentage. The regions are defined in figure 8(K)

structure becomes more profound in the cases with increased vacancy concentration (refer to Fig. 8(F-J)).

3.4.2 Defective DWCNTs under tension

Similar to compression, the regionally defective DWCNTs are axially stretched further to observe the localized shape changes; but unlike the compression cases, the shape modulations are not visually evident in the radial direction. To explore it more thoroughly we capture the center of mass of the atoms to extract the movement of atoms in the lateral dimensions of loading with respect to the length of the whole structure. It is evident from the results that the

region in the vicinity of the fixed ends does not reveal significant changes in the lateral movement of atoms(refer to Figs. 9(A, E) and 10(A, E)), whereas in all the other cases a considerable movement of atoms in x and y direction is observed in the defective regions with the increasing strain (refer to the Figs. 9 and 10). It is also evident from the results of tensile deformation that the cases with a 0.5% single vacancy concentration (Fig. 10) show the movement of atoms with higher magnitudes than the cases with a single atomic vacancy (Fig. 9).

Noteworthy here is that the location and degree of the bulging can be controlled by the appropriate placement of defects in both the cases of compressive and tensile loading. For a particular defect configuration, it can further be programmed (Sinha and Mukhopadhyay 2023) as a function of applied far-field displacement. The proposed approach of defect-engineering can be extended to create multiple programmable bulges (leading to spatio-mechanical shape morphing) by simultaneously introducing defects in multiple regions of the nanotube with variable intensity. Such artificial defect engineering could play a important role in the development of nanomechanical devices and systems for far-field actuation and control of various non-uniform span-wise deformation components and transport phenomena at the nanoscale.

4. Summary and perspective

Owing to extreme operating conditions of the synthesis process of CNT nanostructures, they are often imposed with certain inevitable structural deformities such as single vacancy and nanopore defects. These random irregularities limit the intended functionalities of carbon nanotubes severely. In the present study, we have investigated the spatio-mechanical behaviour of DWCNT under the influence of inevitable random defects based on molecular dynamics simulations.

Before investigating a range of scenarios of random damages, we have first reported the number of walls, temperature, strain rate dependent fracture, and elastic behaviour of MWCNTs to characterize the critical mechanical properties comprehensively. It is found that the increase in the number of walls of MWCNTs increases the fracture strength. The temperature-dependent analysis reveals that increasing the temperature from 100K to 1200K drastically reduces the failure and elastic characteristics of DWCNT, irrespective of the edge conditions (armchair or zigzag). With respect to the strain rate dependent analysis, it is concluded that irrespective of the chiral conditions, the increase in strain rate has a minor effect on the failure and elastic properties of DWCNT. Subsequently, to explore the inevitable defects inclusion in the nano-structures, we have considered different possible scenarios of randomly distributed single vacancy and nanopore defects in the DWCNT structure. The separate cases of the defective outer wall, inner wall, and multiple walls are analyzed comprehensively to portray the wall-specific vulnerabilities of DWCNT. It is found that the randomly distributed defects in the inner wall have a much more severe effect on the mechanical behaviour of DWCNT in comparison with the deformities with the same concentration in the outer wall. Furthermore, to assess the compound effect of both the defects on the failure and elastic characteristics of DWCNT, a 0.5% concentration of compound defects is first imposed in the inner and outer wall of the DWCNT separately, followed by a 0.25% concentration of compound defects in both walls of the DWCNT. The findings reveal that the mechanical behaviour of DWCNT imposed with compound defects in the outer wall is less critical than in the case of the inner wall and both walls. In general, from the extensive molecular simulations, it is established that the nanopore defects have more detrimental effects on the mechanical behaviour of DWCNT.

In the next stage of the analysis, we have explored the idea of local shape modulation through defect-engineering in the tubular structures under far-field actuation. The DWCNT nanostructure is divided into multiple regions and the defects are imposed region-wise in the outer wall with two different concentrations for this purpose. It is observed that a bulging-induced programmable shape change can be realized as a function of the damage location and intensity along with the possibility of non-uniform deformation control along the longitudinal direction. This approach of defect-engineering can further be extended to create multiple programmable bulges (leading to spatio-mechanical shape morphing) by simultaneously introducing defects in multiple regions of the nanotube with variable intensity. Such artificial defect engineering based on the novel concept of correlating region-wise defects and localized shape modulation could play a crucial role in the development of nanomechanical devices and systems for far-field actuation and control of various non-uniform span-wise deformation components and transport phenomena at the nanoscale.

5. Conclusions

This article investigates the spatio-mechanical behaviour of DWCNT under the influence of inevitable random defects based on molecular dynamics simulations. We have addressed the dual aspect of characterizing the influence of inevitable spatially random defects on a range of critical mechanical properties of CNTs and prospective defect-induced region-wise shape modulation and deformation control (defect engineering). The presented comprehensive numerical results here would lead to an improved understanding of the spatio-mechanical response (/ programming) of CNTs for prospective applications in a range of nanoelectromechanical systems and devices.

Acknowledgment

TM would like to acknowledge the support received through the Science and Engineering Research Board (Grant no. SRG/2020/001398), India.

References

Barber, A.H., Andrews, R., Schadler, L.S. and Wagner, H.D.

(2005), "On the tensile strength distribution of multiwalled carbon nanotubes", *Appl. Phys. Lett.*, **87**(20), 203106. https://doi.org/10.1063/1.2130713

Bedi, D., Sharma, S. and Tiwari, S.K. (2022), "Effect of chirality and defects on tensile behavior of carbon nanotubes and graphene: Insights from molecular dynamics", *Diamond Relat. Mater.*, **121**, 108769. https://doi.org/10.1016/j.diamond.2021.108769

Chandra, Y., Adhikari, S., Mukherjee, S. and Mukhopadhyay, T. (2022), "Unfolding the mechanical properties of buckypaper composites: Nano to macro scale coupled atomistic-continuum simulations", *Eng. Comput.*, 1-31. https://doi.org/10.1007/s00366-021-01538-w

Chawla, R. and Sharma, S. (2017), "Molecular dynamics simulation of carbon nanotube pull-out from polyethylene matrix", *Compos. Sci. Technol.*, **144**, 169-177. https://doi.org/10.1016/j.compscitech.2017.03.029

Chen, W.H., Cheng, H.C. and Liu, Y.L. (2008), "Effects of surface and in-layer van der waals interaction on mechanical properties for carbon nanotubes", *Adv. Mater. Res.*, **33**, 993-998. https://doi.org/10.4028/www.scientific.net/AMR.33-37.993

Chowdhury, S.C. and Okabe, T. (2007), "Computer simulation of carbon nanotube pull-out from polymer by the molecular dynamics method", *Compos. Part A Appl. Sci. Manuf.*, **38**(3), 747-754. https://doi.org/10.1016/j.compositesa.2006.09.011

Cullinan, M.A. and Culpepper, M.L. (2010), "Carbon nanotubes as piezoresistive microelectromechanical sensors: Theory and experiment", *Phys. Rev. B*, **82**(11), 115428. https://doi.org/10.1103/PhysRevB.82.115428

Demczyk, B.G., Wang, Y.M., Cumings, J., Hetman, M., Han, W., Zettl, A. and Ritchie, R.O. (2002), "Direct mechanical measurement of the tensile strength and elastic modulus of multiwalled carbon nanotubes", *Mater. Sci. Eng. A*, **334**(1-2), 173-178. https://doi.org/10.1017/S1431927606062933

Dequesnes, M., Tang, Z. and Aluru, N.R., (2004), "Static and dynamic analysis of carbon nanotube-based switches", *J. Eng. Mater. Technol.*, **126**(3), 230-237. https://doi.org/10.1115/1.1751180

Diao, C., Dong, Y. and Lin, J. (2017), "Reactive force field simulation on thermal conductivities of carbon nanotubes and graphene", *Int. J. Heat Mass Transfer*, **112**, 903-912. https://doi.org/10.1016/j.ijheatmasstransfer.2017.05.036

Dilrukshi, K.G.S., Dewapriya, M.A.N. and Puswewala, U.G.A. (2015), "Size dependency and potential field influence on deriving mechanical properties of carbon nanotubes using molecular dynamics", *Theor. Appl. Mech. Lett.*, **5**(4), 167-172. https://doi.org/10.1016/j.taml.2015.05.005

Dong, J., Salem, D.P., Sun, J.H. and Strano, M.S. (2018), "Analysis of multiplexed nanosensor arrays based on near-infrared fluorescent single-walled carbon nanotubes", *ACS Nano*, **12**(4), 3769-3779. https://doi.org/10.1021/acsnano.8b00980

Eftekhari, M., Mohammadi, S. and Khoei, A. R. (2013), "Effect of defects on the local shell buckling and post-buckling behavior of single and multiwalled carbon nanotubes", *Comput. Mater. Sci.*, **79**, 736-744. https://doi.org/10.1016/j.commatsci.2013.07.034

Ehyaei, J. and Daman, M. (2017), "Free vibration analysis of double walled carbon nanotubes embedded in an elastic medium with initial imperfection," *Adv. Nano Res.*, **5**(2), 179. https://doi.org/10.12989/anr.2017.5.2.179

Eichler, A., Moser, J., Chaste, J., Zdrojek, M., Wilson-Rae, I. and Bachtold, A. (2011), "Nonlinear damping in mechanical resonators made from carbon nanotubes and graphene", *Nature Nanotechnol.*, **6**(6), 339-342. https://doi.org/10.1038/nnano.2011.71

El-Sherbiny, S.G., Wageh, S., Elhalafawy, S.M. and Sharshar, A.A. (2013), "Carbon nanotube antennas analysis and applications", *Adv. Nano Res.*, **1**(1), 13-27. https://doi.org/10.12989/anr.2013.1.1.013

Esfarjani, K., Zebarjadi, M. and Kawazoe, Y. (2006), "Thermoelectric properties of a nanocontact made of two-capped single-wall carbon nanotubes calculated within the tight-binding approximation", *Phys. Rev. B*, **73**(8), 085406. https://doi.org/10.1103/PhysRevB.73.085406

Etesami, M., Nguyen, M.T., Yonezawa, T., Tuantranont, A., Somwangthanaroj, A. and Kheawhom, S. (2022), "3D carbon nanotubes-graphene hybrids for energy conversion and storage applications", *Chem. Eng. J.*, **446**(3), 136370. https://doi.org/10.1016/j.cej.2022.137190

Fan, Q.Q., Qin, Z.Y., Liang, X., Li, L., Wu, W.H. and Zhu, M.F. (2010), "Reducing defects on multiwalled carbon nanotube surfaces induced by low-power ultrasonic-assisted hydrochloric acid treatment", *J. Experim. Nanosci.*, **5**(4), 337-347. https://doi.org/10.1080/17458080903536541

Farazin, A. and Mohammadimehr, M. (2020), "Nano research for investigating the effect of SWCNTs dimensions on the properties of the simulated nanocomposites: a molecular dynamics simulation", *Adv. Nano Res.*, **9**(2), 83-90. https://doi.org/10.12989/anr.2020.9.2.083

Farshad, K., Simyari, M., Hosseini, S.A., Tounsi, A. (2020), "Size dependent axial free and forced vibration of carbon nanotube via different rod models", *Adv. Nano Res.*, **9**(3), 157-172. https://doi.org/10.12989/anr.2020.9.3.157

Fu, C., Chen, Y. and Jiao, J. (2007), "Molecular dynamics simulation of the test of single-walled carbon nanotubes under tensile loading", *Sci. China Series E*, **50**(1), 7-17. https://doi.org/10.1007/s11431-007-0009-1

Gaillard, J., Skove, M. and Rao, A. M. (2005), "Mechanical properties of chemical vapor deposition-grown multiwalled carbon nanotubes", *Appl. Phys. Lett.*, **86**(23), 233109. https://doi.org/10.1063/1.1946186

Genoese, A., Genoese, A. and Salerno, G. (2020), "In-plane and out-of-plane tensile behaviour of single-layer graphene sheets: a new interatomic potential", *Acta Mechanica*, **231**, 2915-2930. https://doi.org/10.1007/s00707-020-02680-0

Ghavamian, A., Rahmandoust, M. and Öchsner, A. (2012), "A numerical evaluation of the influence of defects on the elastic modulus of single and multiwalled carbon nanotubes", *Comput. Mater. Sci.*, **62**, 110-116. https://doi.org/10.1016/j.commatsci.2012.05.003

Gupta, K.K., Mukhopadhyay, T., Dey, S. (2023) "Probing the molecular-level energy absorption mechanism and strategic sequencing of graphene/Al composite laminates under high-velocity ballistic impact of nano-projectiles", *Appl. Surf. Sci.*, **629**, 156502, https://doi.org/10.1016/j.apsusc.2023.156502

Gupta, K.K., Mukhopadhyay, T., Roy, A. and Dey, S. (2020), "Probing the compound effect of spatially varying intrinsic defects and doping on mechanical properties of hybrid graphene monolayers", *J. Mater. Sci. Technol.*, **50**, 44-58. https://doi.org/10.1016/j.jmst.2020.03.004

Gupta, K.K., Mukhopadhyay, T., Roy, A., Roy, L. and Dey, S. (2021a), "Sparse machine learning assisted deep computational insights on the mechanical properties of graphene with intrinsic defects and doping", *J. Phys. Chem. Solids*, **155**, 110111. https://doi.org/10.1016/j.jpcs.2021.110111

Gupta, K.K., Mukhopadhyay, T., Roy, L. and Dey, S. (2021b), "Hybrid machine learning assisted quantification of the compound internal and external uncertainties of graphene: Towards inclusive analysis and design", *Mater. Adv.*, **3**, 1160-1181. https://doi.org/10.1039/D1MA00880C

Gupta, K.K., Roy, L. and Dey, S. (2022), "Hybrid machine-learning-assisted stochastic nano-indentation behaviour of twisted bilayer graphene", *J. Phys. Chem. Solids*, **167**, 110711.

https://doi.org/10.1016/j.jpcs.2022.110711
Haiquan, W., Zandi, Y., Gholizadeh, M., Issakhov, A. (2021), "Buckling of porosity-dependent bi-directional FG nanotube using numerical method", *Adv. Nano Res.*, **10**(5), 493-507. https://doi.org/10.12989/anr.2021.10.5.493
Hanwell, M.D., Curtis, D.E., Lonie, D.C., Vandermeersch, T., Zurek, E. and Hutchison, G.R. (2012), "Avogadro: an advanced semantic chemical editor, visualization, and analysis platform", *J. Cheminform.*, **4**(1), 1-17. https://doi.org/10.1186/1758-2946-4-17
Humphrey, W., Dalke, A. and Schulten, K. (1996), "VMD: visual molecular dynamics", *J. Mol. Graph.*, **14**(1), 33-38. https://doi.org/10.1016/0263-7855(96)00018-5
Iijima, S. (1991), "Helical microtubules of graphitic carbon", *Nature*, **354**(6348), 56-58. https://doi.org/10.1038/354056a0
Jensen, B.D., Wise, K.E. and Odegard, G.M. (2015), "The effect of time step, thermostat, and strain rate on ReaxFF simulations of mechanical failure in diamond, graphene, and carbon nanotube", *J. Comput. Chem.*, **36**(21), 1587-1596. https://doi.org/10.1002/jcc.23970
Jinkins, K.R., Chan, J., Jacobberger, R.M., Berson, A. and Arnold, M.S. (2019), "Substrate-wide confined shear alignment of carbon nanotubes for thin film transistors", *Adv. Electr. Mater.*, **5**(2), 1800593. https://doi.org/10.1002/aelm.201800593
Jones, J. E. (1924), "On the determination of molecular fields. I. From the variation of the viscosity of a gas with temperature", *Proceedings of the Royal Society of London. Series A, Containing Papers of a Mathematical and Physical Character*, **106**(738), pp.441-462. https://doi.org/10.1098/rspa.1924.0081
Jyoti, J. and Singh, B.P. (2021), "A review on 3D graphene–carbon nanotube hybrid polymer nanocomposites", *J. Mater. Sci.*, **56**(31), 17411-17456. https://doi.org/10.1007/s10853-021-06370-7
Khan, W., Sharma, R. and Saini, P. (2016), "Carbon nanotube-based polymer composites: synthesis, properties and applications", *Carbon Nanotubes Curr. Prog. Polym. Compos.* https://doi.org/10.5772/62497
Kinloch, I.A., Suhr, J., Lou, J., Young, R.J. and Ajayan, P.M. (2018), "Composites with carbon nanotubes and graphene: An outlook", *Science*, **362**(6414), 547-553. https://doi.org/10.1126/science.aat7439
Kuznetsov, V.L., Bokova-Sirosh, S.N., Moseenkov, S.I., Ishchenko, A.V., Krasnikov, D.V., Kazakova, M.A., Romanenko, A.I. and Obraztsova, E.D. (2014), "Raman spectra for characterization of defective CVD multiwalled carbon nanotubes", *Physica Status Solidi B*, **251**(12), 2444-2450. https://doi.org/10.1002/pssb.201451195
Li, F., Cheng, H.M., Bai, S., Su, G. and Dresselhaus, M.S. (2000), "Tensile strength of single-walled carbon nanotubes directly measured from their macroscopic ropes", *Appl. Phys. Lett.*, **77**(20), 3161-3163. https://doi.org/10.1063/1.1324984
Li, Y., Wang, Q. and Wang, S. (2019), "A review on enhancement of mechanical and tribological properties of polymer composites reinforced by carbon nanotubes and graphene sheet: molecular dynamics simulations", *Compos. Part B Eng.*, **160**, 348-361. https://doi.org/10.1016/j.compositesb.2018.12.026
Liew, K.M., He, X.Q. and Wong, C.H. (2004), "On the study of elastic and plastic properties of multiwalled carbon nanotubes under axial tension using molecular dynamics simulation", *Acta Materialia*, **52**(9), 2521-2527. https://doi.org/10.1016/j.actamat.2004.01.043
Lindsay, L. and Broido, D.A. (2010), "Optimized Tersoff and Brenner empirical potential parameters for lattice dynamics and phonon thermal transport in carbon nanotubes and graphene", *Phys. Rev. B*, **81**(20), 205441. https://doi.org/10.1103/PhysRevB.81.205441
Liu, Z., Dai, S., Wang, Y., Yang, B., Hao, D., Liu, D. and Huang, J. (2020), "Photoresponsive transistors based on lead-free perovskite and carbon nanotubes", *Adv. Funct. Mater.*, **30**(3), 1906335. https://doi.org/10.1002/adfm.201906335
Liu, Z., Wang, J., Kushvaha, V., Poyraz, S., Tippur, H., Park, S., Kim, M., Liu, Y., Bar, J., Chen, H. and Zhang, X., (2011), "Poptube approach for ultrafast carbon nanotube growth", *Chem. Commun.*, **47**(35), 9912-9914. https://doi.org/10.1039/C1CC13359D
Lv, Q., Wang, Z., Chen, S., Li, C., Sun, S. and Hu, S. (2017), "Effects of single adatom and Stone-Wales defects on the elastic properties of carbon nanotube/polypropylene composites: a molecular simulation study", *Int. J. Mech. Sci.*, **131**, 527-534. https://doi.org/10.1016/j.ijmecsci.2017.08.001
Merino, C.A.I., Sillas, J.L., Meza, J.M. and Ramirez, J.H. (2017), "Metal matrix composites reinforced with carbon nanotubes by an alternative technique", *J. Alloy Compd.*, **707**, 257-263. https://doi.org/10.1016/j.jallcom.2016.11.348
Mielke, S.L., Troya, D., Zhang, S., Li, J.L., Xiao, S., Car, R. and Belytschko, T. (2004), "The role of vacancy defects and holes in the fracture of carbon nanotubes", *Chem. Phys. Lett.*, **390**(4-6), 413-420. https://doi.org/10.1016/j.cplett.2004.04.054
Mortazavi, B., Fan, Z., Pereira, L.F.C., Harju, A. and Rabczuk, T. (2016), "Amorphized graphene: a stiff material with low thermal conductivity", *Carbon*, **103**, 318-326. https://doi.org/10.1016/j.carbon.2016.03.007
Mukherjee, R., Abhay V.T., Datta, D., Singh, E., Li, J., Eksik, O., Shenoy, V.K., Koratkar, N., (2014), "Defect-induced plating of lithium metal within porous graphene networks", *Nature Commun.*, **5**, 1-10. https://doi.org/10.1038/ncomms4710
Mukhopadhyay, T., Ma, J., Feng, H., Hou, D., Gattas, J. M., Chen, Y. and You, Z. (2020), "Programmable stiffness and shape modulation in origami materials: Emergence of a distant actuation feature", *Appl. Mater. Today*, **19**, 100537. https://doi.org/10.1016/j.apmt.2019.100537
Mukhopadhyay, T., Mahata, A., Adhikari, S., Asle Zaeem, M. (2017), "Effective mechanical properties of multilayer nano-heterostructures", *Sci. Rep.*, **7**, 15818. https://doi.org/10.1038/s41598-017-15664-3
Mukhopadhyay, T., Mahata, A., Naskar, S., Adhikari, S. (2020), "Probing the effective Young's modulus of `magic angle' inspired multi-functional twisted nano-heterostructures", *Adv. Theory Simul.*, **3**(10), 2000129. https://doi.org/10.1002/adts.202000129
Nakai, Y., Honda, K., Yanagi, K., Kataura, H., Kato, T., Yamamoto, T. and Maniwa, Y. (2014), "Giant Seebeck coefficient in semiconducting single-wall carbon nanotube film", *Appl. Phys. Express*, **7**(2), 025103. https://doi.org/10.7567/APEX.7.025103
Ogata, S. and Shibutani, Y. (2003), "Ideal tensile strength and band gap of single-walled carbon nanotubes", *Phys. Rev. B*, **68**(16), 165409. https://doi.org/10.1103/PhysRevB.68.165409
Ohnishi, M., Suzuki, K. and Miura, H. (2016), "Effects of uniaxial compressive strain on the electronic-transport properties of zigzag carbon nanotubes", *Nano Res.*, **9**, 1267-1275. https://doi.org/10.1007/s12274-016-1022-0
Omer, C., Uzun, B., Yayli, M.O. (2020), "Frequency, bending and buckling loads of nanobeams with different cross sections", *Adv. Nano Res.*, **9**(2) 91-104. https://doi.org/10.12989/anr.2020.9.2.091
Peng, B., Locascio, M., Zapol, P., Li, S., Mielke, S.L., Schatz, G. C. and Espinosa, H. D. (2008), "Measurements of near-ultimate strength for multiwalled carbon nanotubes and irradiation-induced crosslinking improvements", *Nature Nanotechnol.*, **3**(10), 626-631. https://doi.org/10.1038/nnano.2008.211
Plimpton, S. (1995), "Fast parallel algorithms for short-range molecular dynamics", *J. Comput. Phys.*, **117**(1), 1-19.

https://doi.org/10.1006/jcph.1995.1039
Qian, D., Wagner, and, G.J., Liu, W.K., Yu, M.F. and Ruoff, R.S. (2002), "Mechanics of carbon nanotubes", *Appl. Mech. Rev.*, **55**(6), 495-533. https://doi.org/10.1115/1.1490129
Qian, Z.S., Shan, X.Y., Chai, L.J., Ma, J.J., Chen, J.R. and Feng, H. (2014), "DNA nanosensor based on biocompatible graphene quantum dots and carbon nanotubes", *Biosens. Bioelectr.*, **60**, 64-70. https://doi.org/10.1016/j.bios.2014.04.006
Rafiee, R. and Pourazizi, R. (2014), "Evaluating the influence of defects on the young's modulus of carbon nanotubes using stochastic modeling", *Mater. Res.*, **17**(3), 758-766. https://doi.org/10.1590/S1516-14392014005000071
Rajasekaran, G., Kumar, R. and Parashar, A. (2016), "Tersoff potential with improved accuracy for simulating graphene in molecular dynamics environment", *Mater. Res. Express*, **3**(3), 035011. https://doi.org/10.1088/2053-1591/3/3/035011
Rao, P.S., Anandatheertha, S., Naik, G.N. and Gopalakrishnan, S. (2015), "Estimation of mechanical properties of single wall carbon nanotubes using molecular mechanics approach", *Sadhana*, **40**(4), 1301-1311. https://doi.org/10.1007/s12046-015-0367-5
Rao, R., Pint, C.L., Islam, A.E., Weatherup, R.S., Hofmann, S., Meshot, E.R., ... Hart, A.J. (2018), "Carbon nanotubes and related nanomaterials: critical advances and challenges for synthesis toward mainstream commercial applications", *ACS Nano*, **12**(12), 11756-11784. https://doi.org/10.1021/acsnano.8b06511
Robertson, A.W. and Warner, J.H. (2013), "Atomic resolution imaging of graphene by transmission electron microscopy", *Nano-scale*, **5**(10), 4079-4093. https://doi.org/10.1039/C3NR00934C
Robertson, A.W., Allen, C.S., Wu, Y.A., He, K., Olivier, J., Neethling, J. and Warner, J.H. (2012), "Spatial control of defect creation in graphene at the nano-scale", *Nature Commun.*, **3**(1), 1-7. https://doi.org/10.1038/ncomms2141
Roy, A., Gupta, K.K. and Dey, S. (2022), "Probabilistic investigation of temperature-dependent vibrational behavior of hetero-nanotubes", *Appl. Nanosci.*, 1-13. https://doi.org/10.1007/s13204-022-02487-6
Roy, A., Gupta, K. K., Naskar, S., Mukhopadhyay, T. and Dey, S. (2021), "Compound influence of topological defects and heteroatomic inclusions on the mechanical properties of SWCNTs", *Mater. Today Commun.*, **26**, 102021. https://doi.org/10.1016/j.mtcomm.2021.102021
Salvetat, J.P., Bonard, J.M., Thomson, N.H., Kulik, A.J., Forro, L., Benoit, W. and Zuppiroli, L. (1999), "Mechanical properties of carbon nanotubes", *Appl. Phys. A*, **69**(3), 255-260. https://doi.org/10.1007/s003390050999
Saumya, K., Naskar, S., Mukhopadhyay, T. (2023) "'Magic' of twisted multi-layered graphene and 2D nano-heterostructures", *Nano Futures*, **7**, 032005. https://doi.org/10.1088/2399-1984/acf0a9
Savin, A.V. and Mazo, M.A. (2020), "The COMPASS force field: Validation for carbon nanoribbons", *Physica E: Low Dimension. Syst. Nanostruct.*, **118**, 113937. https://doi.org/10.1016/j.physe.2019.113937
Saxena, K.K. and Lal, A. (2012), "Comparative Molecular Dynamics simulation study of mechanical properties of carbon nanotubes with number of stone-wales and vacancy defects", *Procedia Eng.*, **38**, 2347-2355. https://doi.org/10.1016/j.proeng.2012.06.280
Seifoori, S., Abbaspour, F. and Zamani, E. (2020), "Molecular dynamics simulation of impact behavior in multiwalled carbon nanotubes", *Superlatt. Microstruct.*, **140**, 106447. https://doi.org/10.1016/j.spmi.2020.106447
Sharma, S., Chandra, R., Kumar, P. and Kumar, N. (2013), "Molecular dynamics simulation of carbon nanotubes", *Nanosci. Technol. Int. J.*, **4**(1), 29-45. https://doi.org/10.1615/NanomechanicsSciTechnolIntJ.v4.i1.20
Sinha, P. and Mukhopadhyay, T. (2023) "Programmable multi-physical mechanics of mechanical metamaterials", *Mater. Sci. Eng. R*, **155**, 100745, https://doi.org/10.1016/j.mser.2023.100745
Stukowski, A. (2009), "Visualization and analysis of atomistic simulation data with OVITO–the Open Visualization Tool", *Modell. Simul. Mater. Sci. Eng.*, **18**(1), 015012. https://doi.org/10.1088/0965-0393/18/1/015012
Sun, D.M., Timmermans, M.Y., Tian, Y., Nasibulin, A.G., Kauppinen, E.I., Kishimoto, S., Mizutani, T. and Ohno, Y. (2011), "Flexible high-performance carbon nanotube integrated circuits", *Nature Nanotechnol.*, **6**(3), 156-161. https://doi.org/10.1038/nnano.2011.1
Sun, X. and Wang, Y. (2002), "Mechanical properties of carbon nanotubes", *ASME Int. Mech. Eng. Congr. Expos.*, **36517**, 53-57. https://doi.org/10.1115/IMECE2002-39484
Talukdar, K. and Mitra, A.K. (2012), "A molecular dynamics simulation study for the mechanical properties of different types of carbon nanotubes", *Appl. Nanosci.*, **2**(3), 377-383. https://doi.org/10.1007/s13204-012-0110-z
Tao, F., Liu, N., Wang, S., Qin, C., Shi, S., Zeng, X., Liu, G. (2021), "Research on the dispersion of carbon nanotubes and their application in solution-processed polymeric matrix composites: A review", *Adv. Nano Res.*, **10**(6), 559-576. https://doi.org/10.12989/anr.2021.10.6.559
Tersoff, J. (1988), "Empirical interatomic potential for silicon with improved elastic properties", *Phys. Rev. B*, **38**(14), 9902. https://doi.org/10.1103/PhysRevB.38.9902
Treacy, M.J., Ebbesen, T.W. and Gibson, J.M. (1996), "Exceptionally high Young's modulus observed for individual carbon nanotubes", *Nature*, **381**(6584), 678-680. https://doi.org/10.1038/381678a0
Wang, L., Boutilier, M.S., Kidambi, P.R., Jang, D., Hadjiconstantinou, N.G. and Karnik, R. (2017), "Fundamental transport mechanisms, fabrication and potential applications of nanoporous atomically thin membranes", *Nature Nanotechnol.*, **12**(6), 509.https://doi.org/10.1038/nnano.2017.72
Wang, Q. and Arash, B. (2014), "A review on applications of carbon nanotubes and graphenes as nano-resonator sensors", *Comput. Mater. Sci.*, **82**, 350-360. https://doi.org/10.1016/j.commatsci.2013.10.010
Wong, E.W., Sheehan, P.E. and Lieber, C.M. (1997), "Nanobeam mechanics: elasticity, strength, and toughness of nanorods and nanotubes", *Science*, **277**(5334), 1971-1975. https://doi.org/10.1126/science.277.5334.1971
Xie, S., Li, W., Pan, Z., Chang, B. and Sun, L. (2000), "Mechanical and physical properties on carbon nanotube", *J. Phys. Chem. Solids*, **61**(7), 1153-1158. https://doi.org/10.1016/S0022-3697(99)00376-5
Yang, M., Koutsos, V. and Zaiser, M. (2007), "Size effect in the tensile fracture of single-walled carbon nanotubes with defects", *Nanotechnology*, **18**(15), 155708. https://doi.org/10.1088/0957-4484/18/15/155708
Yao, Z., Zhu, C.C., Cheng, M. and Liu, J. (2001), "Mechanical properties of carbon nanotube by molecular dynamics simulation", *Comput. Mater. Sci.*, **22**(3-4), 180-184. https://doi.org/10.1016/S0927-0256(01)00187-2
Yazdani, H., Hatami, K. and Eftekhari, M. (2017), "Mechanical properties of single-walled carbon nanotubes: a comprehensive molecular dynamics study", *Mater. Res. Express*, **4**(5), 055015. https://doi.org/10.1088/2053-1591/aa7003
Yilmazoglu, O., Popp, A., Pavlidis, D., Schneider, J.J., Garth, D., Schüttler, F. and Battenberg, G. (2012), "Vertically aligned multiwalled carbon nanotubes for pressure, tactile and vibration sensing", *Nanotechnology*, **23**(8), 085501. https://doi.org/10.1088/0957-4484/23/8/085501

Yin, Y., Liu, C. and Fan, S. (2012), "Well-constructed CNT mesh/PANI nanoporous electrode and its thickness effect on the supercapacitor properties", *J. Phys. Chem. C*, **116**(50), 26185-26189. https://doi.org/10.1021/jp3083387

Yousif, M.Y.A., Lundgren, P., Ghavanini, F., Enoksson, P. and Bengtsson, S. (2008), "CMOS considerations in nanoelectron-mechanical carbon nanotube-based switches", *Nanotechnol*., **19**(28), 285204. https://doi.org/10.1088/0957-4484/19/28/285204

Yu, M.F., Lourie, O., Dyer, M.J., Moloni, K., Kelly, T.F. and Ruoff, R.S. (2000), "Strength and breaking mechanism of multiwalled carbon nanotubes under tensile load", *Science*, **287**(5453), 637-640. https://doi.org/10.1126/science.287.5453.637

Yuan, Q., Xu, Z., Yakobson, B.I. and Ding, F. (2012), "Efficient defect healing in catalytic carbon nanotube growth", *Phys. Rev. Lett*., **108**(24), 245505. https://doi.org/10.1103/PhysRevLett.108.245505

Zhang, H., Zhou, Z., Qiu, J., Chen, P. and Sun, W. (2021), "Defect engineering of carbon nanotubes and its effect on mechanical properties of carbon nanotubes/polymer nanocomposites: A molecular dynamics study", *Compos. Commun*., **28**, 100911. https://doi.org/10.1016/j.coco.2021.100911

SR